2018

Regularised Equalisation for OFDM Systems With BEM-Based Channel Estimation

Wei Han
University of Wollongong

Regularised Equalisation for OFDM Systems With BEM-Based Channel Estimation

A thesis submitted in partial fulfilment of the requirements for the award of the degree

Master of Philosophy

from

UNIVERSITY OF WOLLONGONG

by

Wei Han

School of Electrical, Computer and Telecommunications Engineering

August 2018

Statement of Originality

I, Wei Han, declare that this thesis is submitted in partial fulfilment of the requirements for the conferral of the degree Master of Philosophy, from the University of Wollongong, is wholly my own work unless otherwise referenced or acknowledged. This document has not been submitted for qualifications at any other academic institution.

Wei Han

August 30, 2018

Contents

List of Figures

Abbreviations

3G	Third Generation of Wireless Mobile Telecommunications Technology
4G	Fourth Generation of Broadband Cellular Network Technology
5G	Fifth Generation of Digital Cellular Networks Technology
AWGN	Additive White Gaussian noise
BEM	Basis Expansion Model
BER	Bit Error Rate
CE-BEM	Complex-Exponential BEM
CP	Cyclic Prefix
CRB	Cramer-Rao Bound
CSI	Channel States Information
DFT	Discrete Fourier Transform
DSL	Digital Subscriber Line
FBMC	Filter Bank Multi-Carrier
FD	Frequency Domain
FDKD	Frequency-Domain Kronecker Delta
FDM	Frequency-Division Multiplexing
FIR	Finite-Impulse Response
GCE-BEM	Generalized Complex-Exponential BEM
GFDM	Generalised Frequency Division Multiplexing
GPS	Global Positioning System
ICI	Inter-carrier Interference
IDFT	Inverse Discrete Fourier Transform
ISI	Inter-symbol Interference
LOS	Line-of-Sight
LS	Least Square
LTE	Long-Term Evolution
MAP	Maximum-a-posteriori
MLSE	Maximum Likelihood Sequence Estimation
MSE	Mean-Square Error
MMSE	Minimum Mean-Square Error
OFDM	Orthogonal Frequency-Division Multiplexing
QAM	Quadrature Amplitude Modulation
QPSK	Quadrature Phase Shift Keying
SIC	Successive Interference Cancellation

SNR	Signal-to-Noise Ratio
SQRD	Sorted QR Decomposition
TV-Channel	Time-Varying Channel
ZF	Zero Forcing

Abstract

Over the last few decades, wireless communication systems have extraordinary development. Great research efforts have been committed, and a huge amount of incredible outcomes have been made. One of the most challenging issues is how to improve the efficiency of transmission when channel is not stationary and varies with time.

This thesis studies the channel estimation and equalisation of orthogonal frequency-division multiplexing (OFDM) systems over doubly selective channels. We consider practical channel estimation schemes based on the basis expansion model (BEM) and clustered pilots. We investigate the influence of the parameters of the channel estimation scheme, including the dimensionality of the BEM basis and bandwidth chosen for the frequency-domain (FD) channel matrix. We address the performance degradation of linear and non-linear equalisation due to imperfect channel estimation. We study the usage of regularisation techniques to enhance the performance of both linear and non-linear equalisation schemes. We also consider reduced-complexity segment-by-segment implementations. The numerical results show that regularisation can effectively enhance the detection performance.

Notation: We use upper and lower-case boldface letters to denote matrices and column vectors. $(\cdot)^{(t)}$ denotes matrix or vector in the time domain. $(\cdot)^*$, $(\cdot)^T$ and $(\cdot)^H$ represent conjugate, transpose and complex conjugate transpose (Hermitian), respectively. $\mathbb{E}\{\cdot\}$ stands for expectation and $Q[\cdot]$ denotes hard decision. $\otimes$ and $\odot$ represent the Kronecker product and the Schur-Hadamard (elementwise) product, respectively. $(\cdot)^\dagger$ represents pseudoinverse. We denote the $M \times N$ all-zero matrix as $\mathbf{0}_{M\times N}$, and the identity matrix as $\mathbf{I}$.

Acknowledgments

First of all, I would express my sincerest gratitude to my supervisor Dr. Jun Tong, for his patient guidance, constructive suggestions and constant encouragement through master studies. Regarding my special experience in the last 5 years, I will never be able to achieve the target without his help. He is my mentor in both research and life.

Special thanks for my co-supervisor Dr. Qinghua Guo for all your support and guidance since the beginning. I am likewise grateful to my research group member Tianle Liu for his insightful discussion and invaluable help through the tough time.

Finally, I wish to express my sincere appreciation to my family for their great support and love throughout my life. It is not possible for me to reach this stage without their support.

Chapter 1

Introduction

1.1 Background

Over the past few decades, wireless communication systems have been widely used through the applications such as mobile phones, GPS, Wi-Fi, and Bluetooth. With the evolution of wireless communication systems, new applications and services are extraordinarily penetrating into people's daily lives. It is well established that orthogonal frequency division multiplexing (OFDM) is one of the key technologies for wideband digital communications, which has been widely used in different systems, such as digital television and audio broadcasting, DSL Internet access, wireless networks, and power-line communications [1] [2]. In the recent past, many new methods are built on the common fundamental principle of OFDM to meet the challenging needs of 5G, such as filter bank multi-carrier (FBMC) and generalised frequency division multiplexing (GFDM) [3].

However, the huge growth of both applications and users will require more powerful and reliable wireless communication systems. The system should be robust and vigorous under mobility environments. A relevant practical application is about the global requirement for wireless communications under high

speed scenarios, where the speed of trains can reach up to 380 km/h for commercial purpose [4]. Compared to the general circumstances in OFDM systems, one of the challenging issues in high speed wireless communication systems is the variation of communication channel caused by the large Doppler spread. Based on the example above, assuming that the carrier frequency is $f_c = 2.16$ GHz, the maximum Doppler frequency could be $f_d = 760$ Hz. Due to multipath propagation and Doppler spread, transmitted signals under high mobility scenarios will experience fading and distortion, which may lead to high bit error rate (BER) and may be a concern for the reliability and effectiveness of mobile communication systems.

OFDM has the advantages of low-complexity frequency-domain equalisation and flexible resource allocation in frequency-selective channels. However, one of the main challenges of OFDM in practice is its high sensitivity to Doppler spreads, which may be caused by movements of the transmitter or receiver. Such Doppler spreads lead to corruption of the orthogonality among the sub-carriers and induce inter-carrier interference (ICI). This poses challenges for pilot-assisted channel estimation due to the mixing of pilot and information-carrying data across the sub-carriers [5], [6]. Furthermore, single-tap equalisation is no longer optimal for signal recovery.

The number of channel coefficients estimated is significantly increased for OFDM in doubly selective channels due to time variation. The parameters used to represent these channel statistics are usually based on physical propagation parameters such as the path delay, path frequencies, path angles of arrival, etc. A common approach is to describe the channel taps statistically by a channel model

from existing works.

A useful approach to reduce the number of parameters to be estimated during channel estimation is basis expansion model (BEM), which represents the time series of different channel tap coefficients on a given set of basis, such that a reduced number of free parameters are sufficient to approximate the time-varying channel coefficients. As a consequence, the pilot overhead can be reduced. Such BEM may be constructed from channel statistics, such as complex-exponential BEM (CE-BEM). Generalised complex-exponential BEM (GCE-BEM) may be used as well, which employs a set of complex exponentials that are more closely spaced in the frequency domain than CE-BEM.

1.2 Research Motivations and Objectives

Channel estimation and equalisation are essential for achieving high performance of wireless communication systems. During the last 20 years, a number of approaches have been developed for channel estimation and equalisation.

The tasks at the receiver side include the estimation of the frequency-domain channel matrix and the recovery of the transmitted signal. In this thesis, we will investigate the choice of the dimensionality of the BEM and bandwidth of the frequency-domain channel estimate, which have significant impact on the quality of channel estimation and equalisation and also the complexity of the signal processing algorithms. We will also investigate the design of equalisers. We show that the widely used zero-forcing (ZF) equaliser suffers from significant error floors when the ICI is significant. We show that the regularisation technique can be used to effectively lower such error floor. We also show that regularisation

can be combined with the nonlinear decision feedback equaliser (DFE) based on sorted QR decomposition (SQRD). Equalisation in a segment-by-segment manner can further reduce the complexity without compromising performance.

The numerical results indicate that for given basis dimensionality and bandwidth, regularisation can significantly improve the equalisation performance.

1.3 Thesis Organisation

The organisation of this thesis shows as follows

- Chapter 2 first introduces the principle of OFDM systems and the time-varying channel model. Then, it gives a review of existing BEM models, channel estimation schemes and equalisation methods,
- Chapter 3 describes the system model and simulation set, then we discuss the influence of the selection of BEM dimension and channel bandwidth,
- Chapter 4 introduces DFE to BEM based OFDM systems, then proposes adapted regularisation and segment-by-segment equalisation for both linear and non-linear systems,
- Chapter 5 summarises this thesis and addresses the planned and possible directions for further work.

1.4 Publications

1. W. Han, J. Tong, Q, Guo, J. Xi, Y. Yan, "Regularised Equalisation for OFDM Systems With BEM-Based Channel Estimation", in 9-th International Conference on Wireless Communications and Signal Processing, WCSP 2017,

pp.1-6

Chapter 2

Literature Review

2.1 Introduction

This chapter introduces the system model. Firstly, we give an introduction to multi-path channel propagation. Then, we show the large-scale and small-scale effects which include multi-path and Doppler spread. Next, we discuss fading channel classification and introduce doubly selective channel. After that, we give an introduction of Orthogonal Frequency Division Multiplexing (OFDM) system and time varying channel models. In addition, Basis Expansion Model (BEM) method is included. Then, we compare the performance between existing equalisers and channel estimators. We also discuss our objectives of this study, i.e., to investigate and optimise the performance of channel estimation and equalisation methods for OFDM systems.

2.2 Time Varying Multi-path Channel

2.2.1 Radio Wave Propagation

In wireless communication, radio wave propagation is affected by the wireless channel in which they travel and in particular the way they propagate around

the Earth in various parts of the atmosphere. Compared with the stationary and predictable wired channel, a wireless channel is extremely random and presents severe effects for a wireless communications system. These include distortions, noises, interferences and other impediments which are time-varying and unpredictable as a result of the velocity for transmitter or receiver [1]. During the propagation through the wireless channel, the signal suffers from path loss and fading. In general, radio wave propagation has large-scale effects and small-effects on the received signal:

- Large-scale Effects

  The large-scale propagation effects are used to describe variations in the received signal power due to the complex environment in suburbs as well as the density and height of buildings in urban areas. It can be characterised by path loss and shadowing. Path loss characterises the decrease of the power of the transmitted signal due to the increased travel distance. Shadowing is due to large objects, such as buildings or mountains, which attenuates the signal power through reflection, diffraction and scattering [1]. Large-scale effects are significant for predicting the coverage and availability of services [7].

- Small-scale Effects

  The small-scale propagation effects are used to characterise the rapid variations of the amplitudes, phases and delays of a transmitted signal over a short period of time or a short distance [8]. Two main reasons that caused small-scale fading are time dispersion due to multi-path and frequency dis-

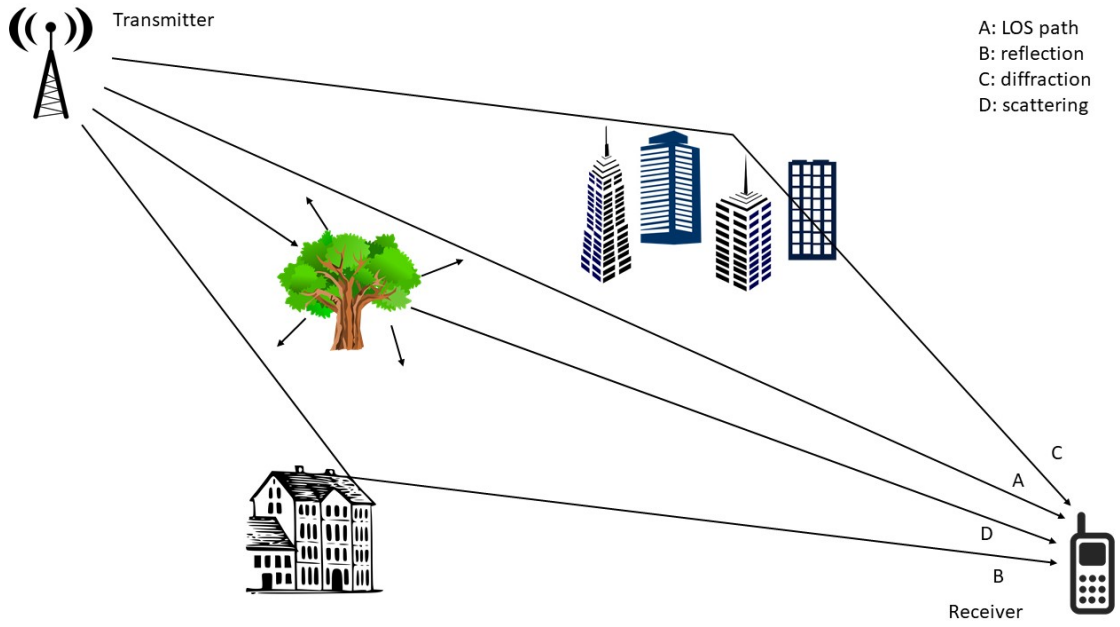

Figure 2.1: Multi-path channel propagation

persion due to Doppler spread [7].

2.2.2 Multi-path Propagation

In wireless communications, the waves may travel from the source to the receiver through a direct path, which is called line-of-sight (LOS) propagation. However, waves may be diffracted, refracted, reflected, or absorbed by the atmosphere and obstructions with material and generally cannot travel through obstacles, as shown in Fig.2.1. Hence, the propagation paths from the transmitter to the receiver could be multiple. As a result, multiple copies of the same transmitted signal can be observed with different delays, angle or arrivals, and gains after reflection, diffraction and scattering. The superposition of the signals can be constructive and destructive, leading to significant fluctuations of the signal observed. This leads to the multi-path fading effect [8].

As a result of different delays of multi-path propagation, the received signal has a longer duration than the transmitted signal, which introduces delay spread

into received signal [7]. The delay spread is a characteristic of the time difference between the first received LOS component or multi-path component, and the last received multi-path component. Multi-path delay spread introduces frequency selective fading and inter-symbol interference (ISI). Frequency selective fading means that the channel does not affect all frequency components of the signal equally [7]. Certain frequency components in the received signal spectrum have greater gains than others. Both fading and interference could lead to signal distortions and quality degradations of wireless communication systems.

The time dispersion of channel can be described by delay spread and coherence bandwidth. The delay spread can be quantified by a root mean square delay spread σ_τ. The inverse of the root mean square delay spread is called coherence bandwidth, represented by B_c. The coherence bandwidth is a statistical measure of the frequency range over which a channel affects the signal spectrum, in the same way, causing an approximately constant attenuation and linear change in phase [8].

2.2.3 Doppler Shift

In mobile communications, high speeds of transmitter or receiver will cause the change in frequency of a wave for an observer moving relative to the source of the wave, which is also called Doppler shift. As Fig.2.2 shows, let us assume that a receiver inside of a vehicle is moving at a constant velocity v from point A to B. For a signal transmitted from S, the phase change at receiver side is given as

$$\Delta\phi = \frac{2\pi v \Delta t}{\lambda} \cos\theta \tag{2.1}$$

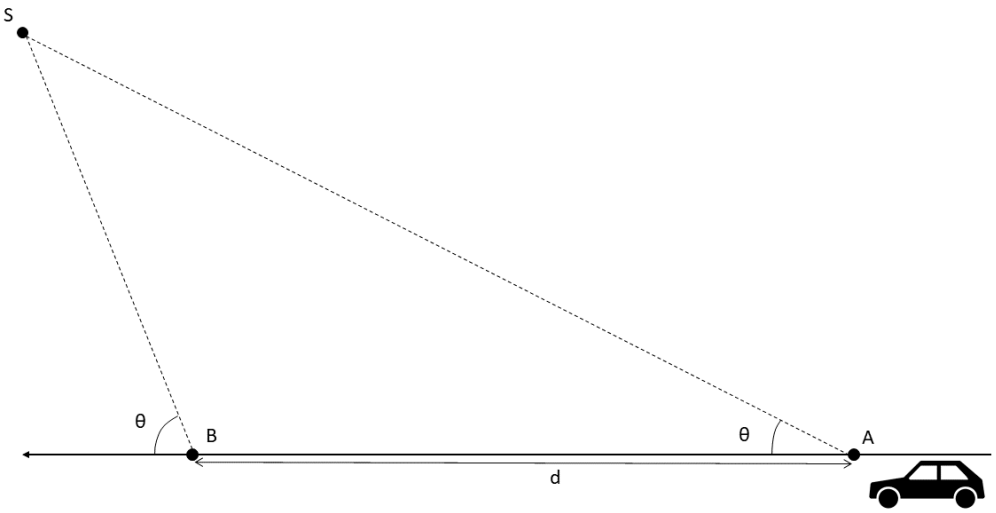

Figure 2.2: Illustration of Doppler shift

where Δt is the time duration for vehicle to move from A to B. λ is the radio wave length and $\lambda = c/f_c$. c is the speed of light and f_c is the carrier frequency. When the transmitter S is far enough, θ for both A and B can be regarded as the same. Then the Doppler shift can be given as

$$f = \frac{1}{2\pi} \cdot \frac{\Delta\phi}{\Delta t} = \frac{v f_c}{c} \cos\theta. \tag{2.2}$$

The maximum Doppler frequency can be represented as

$$f_d = \frac{v f_c}{c} \tag{2.3}$$

Due to the multi-path propagation, transmitted signals arrive at the receiver through a different path, and this causes Doppler spread of the received signal. For OFDM systems, Doppler spreads lead to corruption of the orthogonality among the sub-carriers and induce inter-carrier interference (ICI). In the wireless channel, as a result of different Doppler shift experienced by the multi-path components, the received signal has a larger bandwidth than that of the transmitted signal.

2.3 Channel Model

In wireless communications, channel state information (CSI) describes how a signal propagates between the transmitter and the receiver. The knowledge of CSI represents the combined effect of, for example, scattering, fading and power decay with distance. The CSI is necessary for recovery information at the receivers side.

2.3.1 Channel Fading

Consider an OFDM system with N_s subcarries, we denote the discrete time-domain transmit signal by $\mathbf{x}^{(t)}$, and the discrete time-domain received signal by $\mathbf{y}^{(t)}$.

Then the CSI could be represented by a discrete time-domain channel matrix $\boldsymbol{H}^{(t)}$. The time-domain transmit-receive signal relation is given by,

$$\mathbf{y}^{(t)} = \mathbf{H}^{(t)}\mathbf{x}^{(t)} + \mathbf{n}^{(t)} \tag{2.4}$$

where $\mathbf{n}^{(t)}$ is the channel noise in the time domain.

Assume a channel with maximum channel tap number $L+1$ and a proper cyclic prefix is applied. A general time-domain channel matrix $\mathbf{H}^{(t)}$can be written as

$$\mathbf{H}^{(t)} = \begin{bmatrix} h_{1,1}^{(t)} & 0 & \cdots & h_{L+1,1}^{(t)} & \cdots & \cdots & h_{2,1}^{(t)} \\ h_{2,2}^{(t)} & h_{1,2}^{(t)} & 0 & \cdots & \cdots & \cdots & h_{3,2}^{(t)} \\ \vdots & & \ddots & \vdots & & & \vdots \\ h_{L+1,L+1}^{(t)} & & \cdots & h_{1,L+1}^{(t)} & & & 0 \\ 0 & & & & \ddots & & \vdots \\ \vdots & & & & & \ddots & 0 \\ 0 & \cdots & 0 & h_{L+1,N_s}^{(t)} & \cdots & \cdots & h_{1,N_s}^{(t)} \end{bmatrix} \tag{2.5}$$

where h_{l,n_s} denotes the value of the l-th tap coefficient at the n_s-th sampling period.

Considering the Discrete Fourier Transform (DFT) operator **F** on either side of (2.4), we get the discrete frequency-domain transmit-receive relation as,

$$\mathbf{y} = \mathbf{F}\mathbf{y}^{(t)} = \mathbf{F}\mathbf{H}^{(t)}\mathbf{F}^{H}\mathbf{x} + \mathbf{F}\mathbf{n}^{(t)} = \mathbf{H}\mathbf{x} + \mathbf{n}, \tag{2.6}$$

where $\mathbf{H} = \mathbf{F}\mathbf{H}^{(t)}\mathbf{F}^{H}$ is the frequency domain channel matrix.

2.3.2 Fading Channel Classification

In a multi-path fading channel, the time dispersion and frequency dispersion lead to different distinct effects. These effects are relating to the feature of the channel propagation, transmitted signal and the velocity between transmitter and receiver. The multi-path delay spread causes the flat fading and frequency selective fading, while the Doppler spread causes the fast fading and slow fading.

2.3.2.1 Flat Fading and Frequency Selective Fading

The transmitted signal experience either flat or frequency selective fading due to the time dispersion. The inverse relation between delay spread τ_c and coherence bandwidth B_c is given as $\tau_c = \frac{1}{B_c}$. Flat fading occurs when the bandwidth B_s of the transmitted signal is less than the coherence channel bandwidth B_c. This condition can be also shown as $T_s > \tau_c$, where T_s is the symbol period. In such a case, the mobile channel has a constant gain and linear phase rotation over its bandwidth.

Frequency selective fading occurs when the signal bandwidth is larger than the coherence channel bandwidth. Similarly, the duration of each symbol is less than the delay spread, $B_s > B_c$ or $T_s < \tau_c$. In the frequency domain, the effects of different components of the signal may be different. This leads to distortion at receiver.

2.3.2.2 Slow Fading and Fast Fading

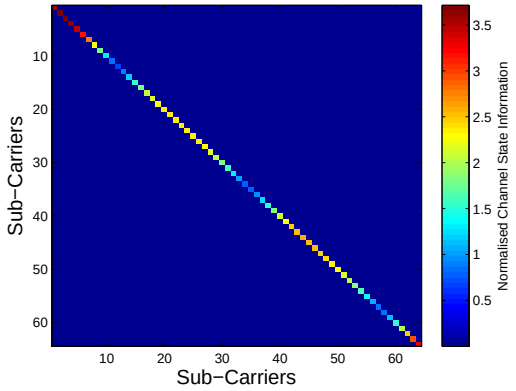

(a) Slow fading channel matrix

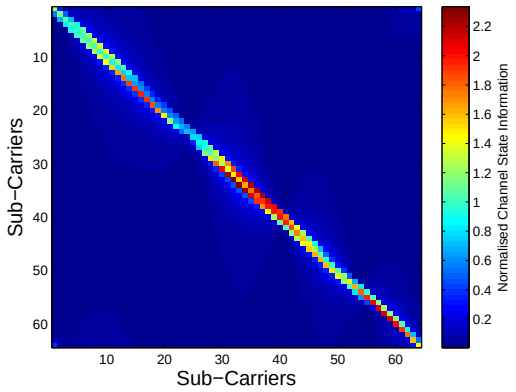

(b) Fast fading channel matrix

Figure 2.3: Examples of channel matrix for slow fading channel and fast fading channel in frequency domain

In the slow fading channel, the rate of channel changes is much slower compared with the transmitted signal. It is almost constant over at least one symbol duration as $T_s < T_c$ or $B_s > \sigma_d$. In the frequency domain, the Doppler spread is less than the bandwidth of the transmitted signal. In such a case, the effects of Doppler spread may be negligible.

Fig.2.3 (a) shows an example of the channel matrix for slow fading channel in frequency domain. h_{l,n_s} is indicated as the elements close to the diagonal line. We can find $\mathbf{H}$ is a diagonal matrix in the frequency domain. In this scenario, simple

channel estimation and equalisation scheme can be used at the receiver to recover the transmit signal **x**.

The Doppler spread causes frequency distortion of propagation signals in a fast fading channel. When the terminal moves fast, the channel impulse response changes rapidly and significantly. The transmitted signal bandwidth is relatively smaller than the Doppler spread in the frequency domain.

In fast fading channels, the effect of Doppler spread becomes critical and causes inter-carrier interference (ICI). Fig.2.3 (b) presents an example of a channel matrix for the fast fading channel. The ICI leads to the spread of the diagonal line to the frequency domain channel matrix, and make it into a banded matrix as the figure shows.

2.3.2.3 Rayleigh Fading

Rayleigh fading is a statistical model for describing the propagation environment of a radio signal. Regarding the central limit theorem, the complex received envelope could be treated as a wide sense stationary complex Gaussian process, as the composite received signal consists of a large number of multi-path components. We can define the received complex envelope by independent and identically distributed random variables $Z_I(t)$ and $Z_Q(t)$, shown as $Z(t) = Z_I(t) + jZ_Q(t)$, where these variables follow Gaussian distribution with zero-means, and variance σ^2. Then the amplitude of the received complex envelope can be represented as $R(t) = \sqrt{Z_I^2(t) + Z_Q^2(t)}$. The amplitude of the received complex envelope follows a Rayleigh distribution [9]

$$P_R(x) = \frac{1}{\sigma^2} x e^{-\frac{x^2}{2\sigma^2}}. \tag{2.7}$$

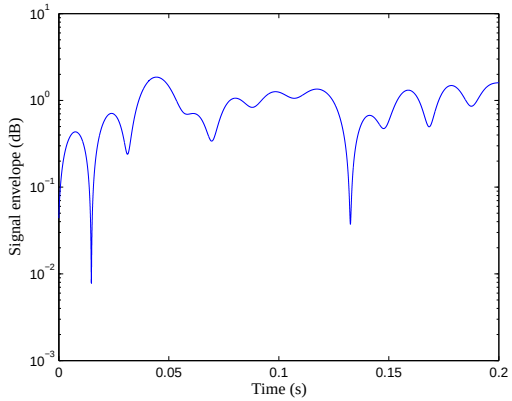

(a) Doppler frequency f_d=30Hz

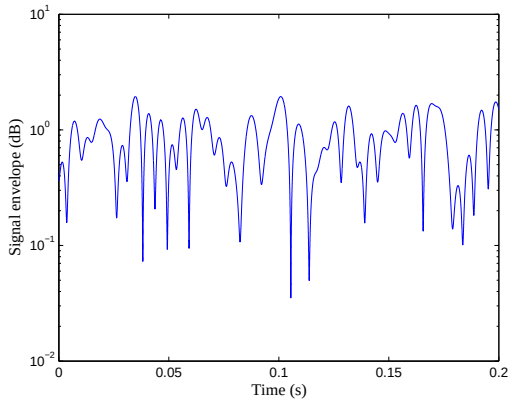

(b) Doppler frequency f_d=100Hz

Figure 2.4: Simulated Rayleigh fading envelope

In radio communications, Rayleigh fading is widely used where the transmitted signal suffers reflection and scattering caused by objects such as buildings or mountains.

Fig.2.4 shows examples of the signal envelope variation of Rayleigh fading channel. Assume the carrier frequency is 1.8 GHz, the Doppler spreads of 30 Hz and 100 Hz, which represent the speeds of 18 km/h and 60 km/h. We can find that the high speed of a terminal can leads to several fades in a small period.

2.3.3 Window Function

Windowing may reduce the amplitude discontinuities at the boundaries of neighboring OFDM symbols. In general, a window function varies smoothly and gradually toward zero at the edges. There are many different types of window functions, which affects differently the frequency spectrum of the signal. Rectangular window is special case where the signal is truncated only.

Another widely used window function is called Hamming Window, which provides an even more significant improvement to the highest sidelobe level. Hamming window is accompanied by a poorer sidelobe roll-off ratio.

2.4 OFDM System

2.4.1 History of OFDM

History of OFDM dates back to 1966 [10], [11]. A significant contribution of OFDM is introducing the Discrete Fourier Transform (DFT) for modulation and demodulation. This efficient processing, eliminates the need of the banks of subcarrier oscillators [12]. However, the system still did not get perfect orthogonality between sub-carriers over a dispersive channel. To figure out this problem, Cyclic Prefix (CP) or cyclic extension is introduced to replace an empty guard space [13].

OFDM is currently used in Digital Audio Broadcasting(DAB), WiMAX, Li-Fi, and ADSL [14]. OFDM, under the name DMT, has also attracted a great deal of attention as an efficient technology for high-speed transmission on the existing LTE and LTE Advanced 4G mobile phone standards. [15]

OFDM is introduced to replace CDMA in the 3G system, as OFDM has several advantages such as ease of implementation, immunity to interference, high data-

rate etc. But OFDM also possesses certain disadvantages like the use of CP, large side lobe which limits the utilisation of the spectrum and which greatly reduced the performance, the loss of bandwidth due to the CP is about 9% in 4G Wi-max. [16]

OFDM system keeps becoming more widely used nowadays because it has plenty of advantages for wireless communications compared with the single-carrier system. The main benefits shown as below [17]:

- multi-path delay spread and channel distortion tolerance.

  The low transmit rate of sub-channels leads to corresponding robustness of OFDM symbols against the ISI due to the multi-path delay spread. Besides, since the bandwidth of each sub-carrier in OFDM is reduced, the amplitude response over that is flat so that a simple equaliser is enough to correct the distortion.

- spectral efficiency

  Since the structure of orthogonal sub-carriers is very dense to save the spectrum, OFDM has better spectral efficiency. Furthermore, using the channel coding technique makes it possible for OFDM to transmit at maximum capacity.

- robustness against impulse noise

  Impulse noise is usually a burst of interference that might cause symbol errors. But OFDM is inherently robust against it since the symbol duration of an OFDM signal is much larger than that of the single-carrier system.

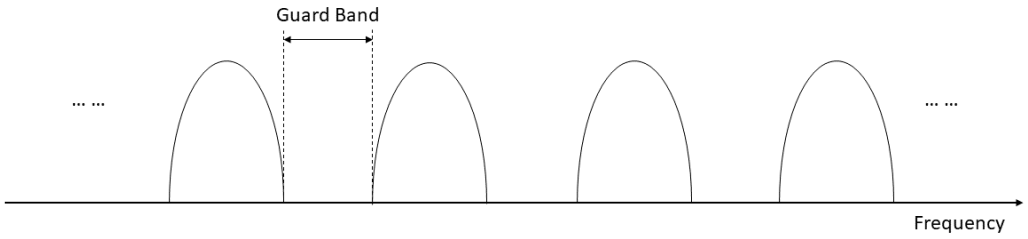

Figure 2.5: Traditional FDM spectrum model

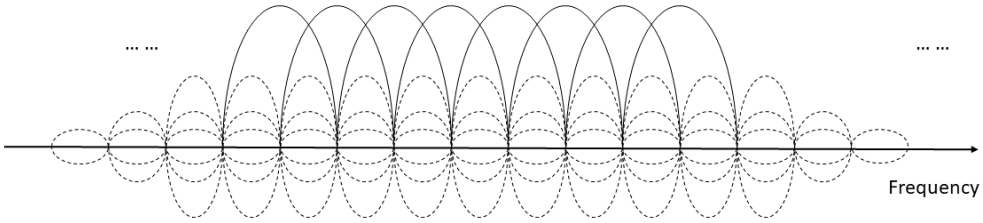

Figure 2.6: OFDM spectrum model

- frequency diversity

  OFDM is the best place to employ frequency diversity. In fact, in a combination of OFDM and CDMA transmission technique frequency diversity is inherently present in the system.

2.4.2 System Model

The basic principle of multi-carrier modulation is to divide the transmitted signal into many different streams transmitted using different sub-channels. Typically, these sub-channels are orthogonal under ideal propagation conditions. The difference between traditional frequency-division multiplexing (FDM) and OFDM could be shown as Fig.2.5 and Fig.2.6. OFDM, similar to FDM, separates the channel bandwidth into multiple narrow-band sub-carriers to carry the information.

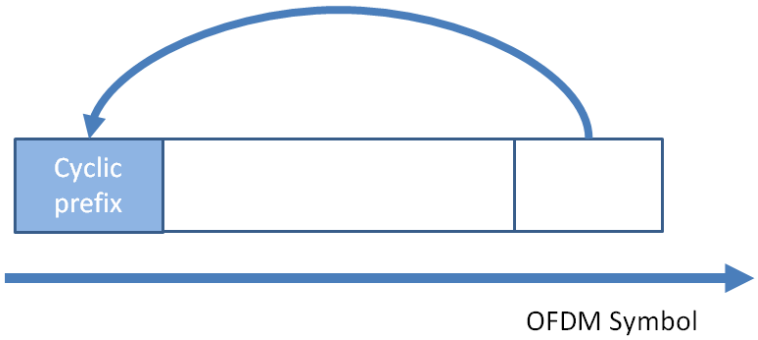

Figure 2.7: The cyclic prefix is a copy of the last part of the OFDM symbol.

To prevent adjacent carrier interference, traditional FDM system inserts guard bands between sub-carriers where can contribute to transmitting data. However, these guard bands can result in a waste of spectrum. To solve this issue, OFDM introduces specific sub-carriers that are all orthogonal to each other. In this case, not only the guard bands can be removed, the sub-carriers can even overlap each other. This is the reason that OFDM is so bandwidth efficient.

A cyclic prefix (CP) is added before each OFDM symbol before transmission to prevent the ISI caused by the propagation in the channel. A CP is a copy of the last part of the OFDM symbol, which is pre-pended to the transmitted symbol, as Fig.2.7 shows [13]. The copy of the end of the current symbol also preserves the orthogonality. As long as the length of the CP is at least same with the length of the multi-path channel, all copies of the current symbol are received before the start of the useful part of the next symbol, thus preventing ISI.

To generate an OFDM symbol, the data to be transmitted is first coded and modulated. Typical modulations include QPSK, 16-QAM, and 64-QAM. This thesis targets on the transmission after coding and employing QPSK as the modulation scheme. As Fig.2.8 shows, the OFDM symbol is divided into N_s parallel streams, where N_s corresponds to the number of the sub-carriers used in the sys-

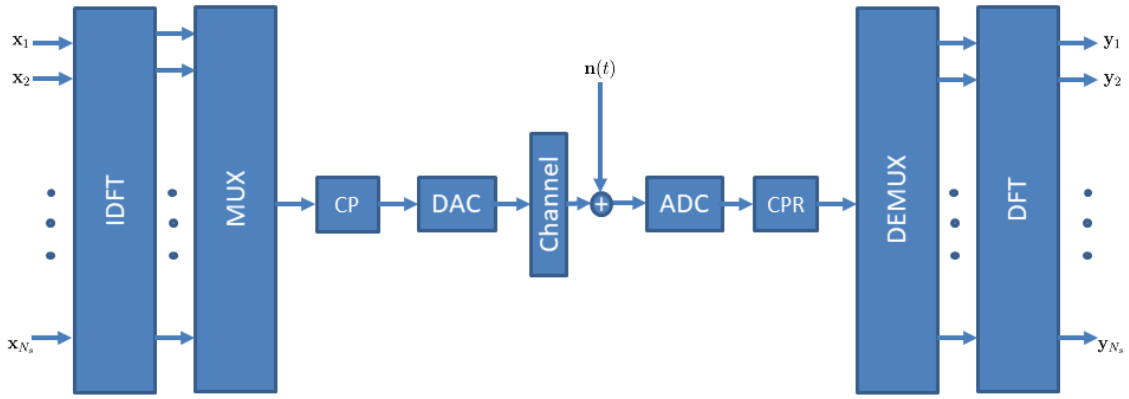

Figure 2.8: A digital implementation of a baseband OFDM system.

tem. A N_s-Point inverse discrete Fourier transform (IDFT) is then used to create the OFDM symbol. The CP is then added at the beginning of the symbol, while the resulting signal is transmitted.

At the receiver side, all the operations performed in the reverse order. One significant difference is a DFT takes the place of IDFT. Some additional processing blocks are required to recover the carrier frequency and the symbol timing synchronisation.

OFDM system is spectrally efficient because of the proximity of the subcarriers. To design a robust system that prevents ISI caused by multi-path propagation and ICI caused by Doppler shift, good knowledge of the channel states information (CSI) is required.

2.5 Basis Expansion Model

One of the main challenges of OFDM in practice is its high sensitivity to Doppler spreads, which may be caused by movements of the transmitter or receiver. Such

Doppler spreads lead to corruption of the orthogonality among the sub-carriers and induce inter-carrier interference (ICI), which will pose challenges for pilot-assisted channel estimation due to the mixing of pilots and information-carrying data across the sub-carriers [5], [6]. Furthermore, single-tap equalisation is no longer optimal for signal recovery.

The number of channel coefficients to be estimated is significantly increased for OFDM in doubly elective channels due to time variation. A useful approach to reduce the number of parameters to be estimated during channel estimation is to adopt the basis expansion model (BEM), which represents the time series of different channel tap coefficients on a given set of basis, such that a reduced number of free parameters are sufficient to approximate the time-varying channel coefficients. As a consequence, the pilot overhead can be reduced.

BEMs have been widely developed to model doubly selective channels in wireless communications, where the time variant impulse responses $h(n_s, l)$ are expressed by the sum of time-varying basis functions. A general BEM expansion of $\boldsymbol{h}(n_s, l)$ can be given as

$$\mathbf{h}(n_s, l) = \sum_{q=0}^{Q} \mathbf{B}_{n_s}(q)\mathbf{c}_l(q) \tag{2.8}$$

where $\mathbf{B}_{n_s}(q)$ gives the value at time n_s of the q-th basis function and $\mathbf{c}_l(q)$ is the coefficient for path l corresponding to the q-th basis function. Q is the dimensionality of BEM basis and $Q + 1$ is the number of basis coefficients. Hence, we can define the basis function in matrix form as

$$\mathbf{B} = \begin{bmatrix} B_{1,1} & \cdots & B_{1,Q+1} \\ \vdots & \ddots & \vdots \\ B_{N_s,1} & \cdots & B_{N_s,Q+1} \end{bmatrix} \tag{2.9}$$

The BEM may be constructed in different ways, e.g., based on channel statis-

tics. Atypical example is the complex-exponential BEM (CE-BEM) [18]. This basis easy to construct but may lead to a large modelling error. The generalised complex-exponential BEM (GEC-BEM) may be used as well, which employs a set of complex exponentials which are more closely spaced in the frequency domain than CE-BEM. Other options include the polynomials-based P-BEM [19], whose performance is somewhat sensitive to the Doppler spread.

2.6 Channel Estimation

2.6.1 Introduction

In wireless communications, the received signal is usually distorted by the propagation channel. To recover the transmitted information, the channel effect has to be estimated and compensated in the receiver. The orthogonality allows each sub-carrier component of the received signal to be expressed as the product of the transmitted signal and channel frequency response at the sub-carrier. In general, the channel can be estimated by using a preamble or pilot symbols known to both transmitter and receiver, which employ various interpolation techniques to predict the channel response of the sub-carriers between pilot tones. In general, data signal as well as the training signal, or both, can be used for channel estimation.

2.6.2 Pilot Assisted Channel Estimation

A pilot is a known sequence in transmitted signal, and it is also called sounding tone, or training sequence. Pilot-based approaches are widely used to estimate the channel and correct the received signal.

Two types of pilot arrangement are demonstrated. In Fig.2.9 block-type pilot arrangement is shown. A whole OFDM block is set as the pilot, which is sent

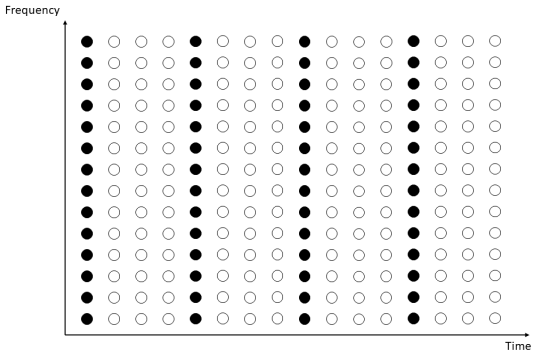

Figure 2.9: Block type pilot arrangement

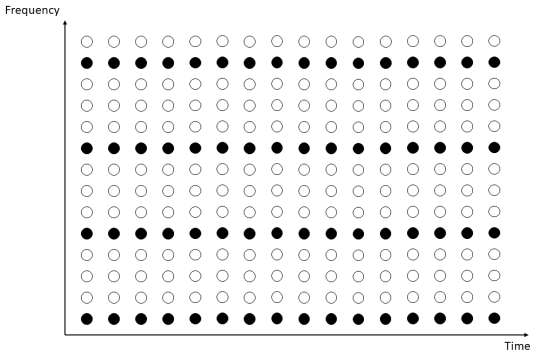

Figure 2.10: Comb type pilot arrangement

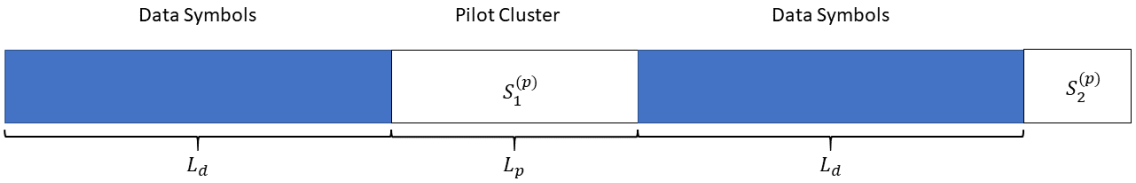

Figure 2.11: OFDM block in frequency domain

periodically in time-domain. This type of pilot arrangement is especially suitable for the slow-fading radio channel. As the training block contains all pilots, channel interpolation in the frequency domain is not required. Therefore, this kind of pilot arrangement is relatively insensitive to frequency selectivity.

Another kind of pilot arrangement is shown in Fig.2.10, referred to as a comb-type pilot arrangement. Pilots uniformly distributed within each OFDM block are used. Assuming that the pilot arrangements are the same, the comb-type pilot arrangement has a higher transmitting rate. The comb-type pilot arrangement system provides better resistance to fast-fading channels. The channel response of non-pilot sub-carriers will be estimated by interpolation neighbouring pilot sub-channels. Thus the comb-type pilot arrangement is sensitive to frequency selectivity when comparing to the block-type pilots.

Due to ISI and ICI, traditional pilot insertion [20] will suffer from interference between information-carrying sub-carriers and pilot sub-carriers in both the time domain and frequency domain. To tackle this challenge, clustered pilots, which are known to both the transmitter and receiver are used. As Fig.2.11 shows, we introduce equi-spaced pilot clusters interlaced with sub-carriers related to transmitted data [21].

2.6.3 Least-Square (LS) Channel Estimation

Currently, the optimal channel estimation methods are based on maximum-a-posteriori (MAP). However, the high complexity makes this method not usefulness in practice. Frequency domain pilot-aided channel estimation techniques are either least-square (LS) based or minimum mean square error (MMSE) based. LS based methods require less computational complexity. Compared with MMSE, the LS channel estimation does not require knowledge of prior channel statistics and noise statistics, and it is widely adopted in practical systems for its simplicity. In high mobility channel estimations, LS combining BEM can be utilised to estimate the channel coefficients in a low dimensional domain. However, it performs inferior when the interference is prominent: we show in the simulation part that the LS estimator suffers from a significant performance gap in comparison with the CramerRao bound (CRB) [5].

Note that, when the channel is in a deep null, the channel noise may get an enhancement. Due to the simplicity, however, the LS method is widely used, and introduced in the proposed system for channel estimation.

2.7 Equalisation

2.7.1 Introduction

In the time-varying channel, delay spread leads to ISI, which in turn produces an irreducible error floor in most digital modulation techniques. In a broad sense, equalisation defines any signal processing technique used at the receiver to alleviate with ISI. During the process of removing ISI, the equaliser design has to avoid that the noise power get enhanced in the received signal.

The optimal equalisation technique to use is the maximum likelihood sequence estimation (MLSE). Unfortunately, the complexity of this technique grows exponentially with memory length and is therefore impractical on most channels of interest. Equalisation techniques fall into two broad categories: linear and non-linear.

2.7.2 Linear Equaliser

The linear equaliser is simple linear filter structures that try to invert the channel in the sense that the product of the transfer functions of channel and equaliser fulfils a particular criterion. This criterion can either be achieving a completely flat transfer function of the channel concatenation or minimising the mean-squared error at the filter output. The linear equalisation methods are generally the simplest to implement and to understand conceptually.

However, linear equalisation typically suffers from noise enhancement on frequency selective fading channels, and are therefore cautious about being used in most wireless applications. The typical linear equaliser used such as zero-forcing equaliser and linear minimum mean square error equaliser.

2.7.3 Non-linear Equaliser

Among non-linear equalisation techniques, decision-feedback equalisation (DFE) has a simple underlying premise: once we have detected a symbol correctly, we can use this knowledge in conjunction with the knowledge of the channel impulse response to compute the ISI caused by detected symbols. However, on channels with low SNR, the DFE suffers from error propagation when symbols are decoded in error, leading to poor performance.

2.7.4 Regularised Equalisation

Regularisation principle has been widely used in ill-posed statistics [22] and inverse problems [23]. It has been proved that regularisation techniques can be applied to improve the robustness of linear equaliser. Efficient implementations using principal components analysis, Krylov subspace expansion and diagonal loading (DL) have been developed [24].

2.8 Conclusion

In this Chapter, we first reviewed the fading channel for OFDM system. The channel estimation based on the BEM model is also discussed in this Chapter. Some existing equalisation schemes are introduced and compared. This thesis aimed to improve the BER performance of OFDM system with BEM-based channel estimation at a low complexity.

Chapter 3

Pilot Assisted Channel Estimation for OFDM System

3.1 Introduction

In this Chapter, we firstly review the system model for the OFDM system with BEM-based channel estimation as we introduced in the last Chapter. We consider LS channel estimation and ZF equalisation. In the literature, parameters of the BEM, channel estimator and equaliser are assumed fixed. In practice, however, the selection of parameters including dimensionality of the BEM basis and bandwidth chosen for FD channel matrix have a significant effect on both performance and complexity. This chapter investigates these issues and reports the observations.

3.2 System Model

3.2.1 OFDM System Model

Considering the transmitted signal in time-domain as

$$\mathbf{x}^{(t)} = \mathbf{F}^H \mathbf{x} \tag{3.1}$$

where $\mathbf{F} \in \mathbb{C}^{N_s \times N_s}$ is the N_s-point discrete Fourier transform (DFT) matrix, whose (p,q)-th entry is given by $[\mathbf{F}]_{p,q} = 1/\sqrt{N_s} e^{-j2\pi pq/N_s}$, the frequency-domain symbol modulated onto N_s carriers is shown as

$$\mathbf{x} \triangleq [x_1, x_2, \ldots, x_{N_s}]^T \in \mathbb{C}^{N_s}. \tag{3.2}$$

With proper cyclic prefix insertion and removal, the received signal in frequency-domain can be written as

$$\begin{aligned} \mathbf{y} &= \mathbf{F}\mathbf{y}^{(t)} \\ &= \mathbf{F}\mathbf{H}^{(t)}\mathbf{F}^H\mathbf{x} + \mathbf{F}\mathbf{n}^{(t)} \\ &= \mathbf{H}\mathbf{x} + \mathbf{n} \end{aligned} \tag{3.3}$$

where

- $\mathbf{y}^{(t)}$ is the received signal in time-domain,
- $\mathbf{n}^{(t)}$ and $\mathbf{n}$ are the time- and frequency-domain additive white Gaussian noise (AWGN) with variance σ^2,
- $\mathbf{H}^{(t)} \in \mathbb{C}^{N_s \times N_s}$ and $\mathbf{H} = \mathbf{F}\mathbf{H}^{(t)}\mathbf{F}^H$ are matrices that contains the channel coefficients in the time and frequency domain, respectively.

In this thesis, we consider a moving terminal with many uniformly distributed scatterers. This causes the typical bathtub-shaped Doppler spectrum [25]. We assume the multi-path channel is a finite-impulse-response (FIR) filter with $L+1$ taps, which are random variables with an exponential power intensity profile, shown as $\mathbf{R}_{mp} = diag\left(\sigma_0^2, \cdots, \sigma_L^2\right)$, where $\sigma_l^2 = e^{-l/10}$.

In this test case, the received signal can be directly inverted with $\mathbf{H}$ to restore the transmitted signal correspondingly. However, $\mathbf{H}$ is generally unknown in practice, the reliable channel statistics obtained by channel estimation exploring.

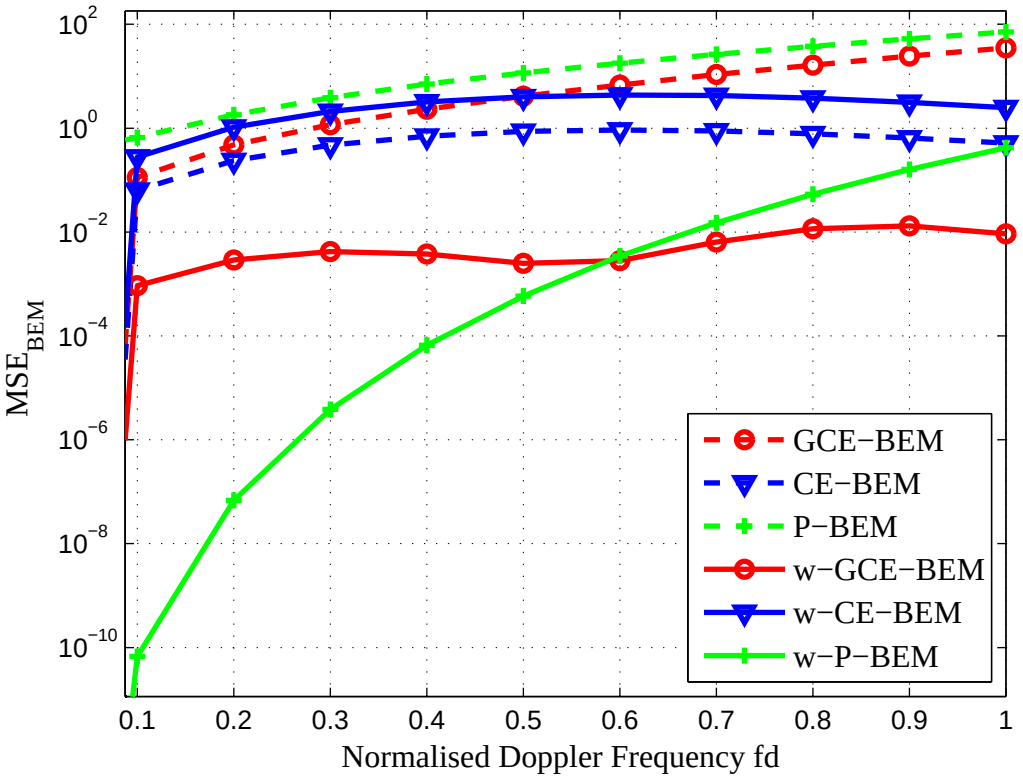

Figure 3.1: Average modelling errors with different BEM bases.

3.2.2 Windowed Channel Model

In order to alleviate the ICI, the window function can be applied at the receiver. The resulting frequency-domain received signal can be rewritten as

$$\mathbf{y} = \mathbf{F}diag\{\mathbf{w}\}\mathbf{H}^{(t)}\mathbf{F}^{H}\mathbf{x} + \mathbf{F}diag\{\mathbf{w}\}\mathbf{n}^{(t)} \tag{3.4}$$

where $\mathbf{w} = [w_1, \cdots, w_{N_s}]^T$ defines the type of the window.

We introduce the time domain window function, Hamming window, into the system as

$$[\mathbf{w}] = \sum_{n_s=0}^{N_s-1} [a_0 + a_1 e^{(-2\pi j n_s/N_s)} + a_1 e^{(2\pi j n_s/N_s)}] \tag{3.5}$$

where a_0 and a_1 are windowing coefficients. In this thesis, these coefficients are given by $a_0 = 1$ and $a_1 = -0.422$.

From now on, we consider all the systems combined with Hamming window function. Only the scenario without windowing will be stressed out.

3.3 BEM Based Channel Estimation

3.3.1 BEM Channel Model

Three different bases, i.e., CE-BEM, GCE-BEM and P-BEM with and without windowing, are compared in Fig.3.1 in terms of $MSE_{BEM} = \mathbb{E}\{\|\epsilon\|^2\}$, where the typical bathtub-shaped Doppler spectrum [25] is assumed for the time-varying channel, and the windowing function is set as the MBAE-SOE window [26]. From the results shown, we can observe that BEMs have small modelling errors at lower Doppler spreads and GCE-BEM is more robust against the Doppler frequency. In the following, we will focus on windowed GCE-BEM with fixed $K_b = 2$.

Different BEM bases can be used. There is also the choice of DKL-BEM [27], which uses a reduced-rank decomposition of the Doppler spectrum. This basis requires the statistics of the channel, which is difficult to obtain in practice. Note that the window $\mathbf{w}$ used at the receiver can be incorporated into the BEM design and the windowed basis matrix is constructed as $\mathbf{B} = diag\{\mathbf{w}\}\tilde{\mathbf{B}}$. When windowing is not considered for the BEM construction, $\mathbf{B} = \tilde{\mathbf{B}}$ is chosen as the original BEM basis matrix [19].

In this thesis, we will target on the windowed GCE-BEM for the high performance and efficiency. However, different types of BEMs shall be considered and compared in further work.

For the l-th tap of the channel, $l = 1, 2, \cdots, L+1$, let $\mathbf{h}_l^{(t)} = [w_1 h_{l,1}^{(t)}, w_2 h_{l,2}^{(t)}, \cdots, w_{N_s} h_{l,N_s}^{(t)}]^T$.

The BEM models the time-varying channel coefficients by

$$\mathbf{h}_l^{(t)} = \mathbf{B}\mathbf{c}_l + \epsilon_l, \tag{3.6}$$

i.e.,

$$\begin{bmatrix} h_{l,1}^{(t)} \\ \vdots \\ h_{l,N_s}^{(t)} \end{bmatrix} = \begin{bmatrix} b_{1,1} & \cdots & b_{Q+1,1} \\ \vdots & & \vdots \\ b_{1,N_s} & \cdots & b_{Q+1,N_s} \end{bmatrix} \begin{bmatrix} c_{l,1} \\ \vdots \\ c_{l,Q+1} \end{bmatrix} + \begin{bmatrix} \epsilon_{l,1} \\ \vdots \\ \epsilon_{l,N_s} \end{bmatrix}, \tag{3.7}$$

where $\mathbf{B} \in \mathbb{C}^{N_s \times (Q+1)}$ is the basis matrix that collects $Q+1$ basis functions $\mathbf{b}_q$, $\mathbf{c}_l$ is a coefficient vector of length $Q+1$, and ϵ_l is the corresponding BEM modelling error.

For the length-$(L+1)N_s$ vector

$$\mathbf{h}^{(t)} \triangleq \left[w_1 h_{1,1}^{(t)}, \cdots, w_1 h_{1,L+1}^{(t)}, \cdots, w_{N_s} h_{N_s,1}^{(t)}, \cdots, w_{N_s} h_{N_s,L+1}^{(t)}\right]^T$$

which collects all the tap coefficients, we can further show that

$$\mathbf{h}^{(t)} = \left(\mathbf{B} \otimes \mathbf{I}_{L+1}\right) \mathbf{c} + \boldsymbol{\epsilon}, \tag{3.8}$$

where $\mathbf{c}$ is a length-$(Q+1)(L+1)$ vector collecting all the BEM coefficients and ϵ is the modelling error. Given the basis matrix $\mathbf{B}$, the channel is characterized by the BEM coefficients $\mathbf{c}$.

3.3.2 Data Model

Considering the BEM modelled channel, we can describe the OFDM system model by substituting (3.8) in (3.3). The frequency-domain system model can now be given as

$$\mathbf{y} = \sum_{q=1}^{Q+1} \mathbf{D}_q \boldsymbol{\Delta}_q \mathbf{x} + \mathbf{n} + \boldsymbol{\delta} \tag{3.9}$$

where $\mathbf{n}$ and δ are the noise and error due to BEM modelling error, respectively. $\mathbf{D}_q$ is a circulant matrix whose first column is the frequency response of the q_{th} basis

function, i.e., $\mathbf{D}_q \triangleq \mathbf{F} diag\left\{\mathbf{b}_q\right\}\mathbf{F}^H$. $\mathbf{\Delta}_q$ denotes a diagonal matrix whose diagonal is the frequency response of the BEM coefficients corresponding to the q-th basis function, i.e., $\mathbf{\Delta}_q \triangleq diag\left\{\mathbf{F}_{L+1}\left[c_{q,1}, \cdots, c_{q,L+1}\right]^T\right\}$, where $\mathbf{F}_{L+1}$ denotes the first $L+1$ columns of the matrix $\sqrt{N_s}\mathbf{F}$.

For time-invariant channels, $\mathbf{D}_q$ becomes a scaled identity matrix. But in TV channels, the non-diagonal entries of $\mathbf{D}_q$ are no longer zeros.

Before we move further, we will make three assumption as shown below:

- Assumption (1):

  time-domain noise is assumed to be zero-mean white Gaussian with variance σ_n^2;

- Assumption (2):

  the transmitted data $\boldsymbol{x}^{(d)}$ are assumed to be zero-mean white with variance σ_d^2 and uncorrelated with channel noise $\boldsymbol{n}$, i.e., $\mathbb{E}\left\{\boldsymbol{x}^{(d)}\boldsymbol{n}^H\right\} = 0$;

- Assumption (3):

  in channel estimation, the BEM approximation is assumed holding perfectly. Then the modelling errors of BEM could be ignored, which means $\boldsymbol{\epsilon} = 0$ and $\boldsymbol{\delta} = 0$.

These assumptions are motivated by the fact that we will mainly focus on the channel estimation and equalisation based on BEMs that allow for a satisfactory fit. As Fig.3.1 shows, BEMs capture the TV channels adequately with minor modelling errors. The residual modelling errors combine into system errors.

From (3.9), we estimate the $(L+1)(Q+1)$ BEM coefficients in $\boldsymbol{c}$ instead of the estimating the channel matrix $\boldsymbol{H}$ directly. We assume that M_p pilot clusters of

length L_p, denote as $\boldsymbol{x}_m^{(p)}, m = 0, 1, \cdots, M_p - 1$, are added into transmitted signal. As indicated in Fig.2.11, all these pilot clusters stacked form the pilot vector $\boldsymbol{x}^{(p)} \triangleq \left[\boldsymbol{x}_1^{(p)}, \cdots, \boldsymbol{x}_{M_p}^{(p)}\right]^T$. These pilot clusters are interleaved by data symbols $\boldsymbol{x}^{(d)}$. For a time-varying OFDM system, it is not clear that what is the optimal pilot placement. Following [20], equidistant pulse-shaped pilot clusters are optimised based on GCE-BEM assumption. In this work, we focus on equidistant pulse-shaped pilot cluster.

3.3.3 LS Estimation

At the receiver side, we collect the frequency-domain symbols $\mathbf{y}^{(p)}$ on sub-carriers which are related to the pre-known pilot clusters, as shown below

$$\mathbf{y}^{(p)} = \sum_{q=1}^{Q+1} \mathbf{D}_q^{(p)} \boldsymbol{\Delta}_q^{(p)} \mathbf{x}(d) + \sum_{q=1}^{Q+1} \mathbf{D}_q^{(d)} \boldsymbol{\Delta}_q^{(d)} \mathbf{x}(d) + \mathbf{n}^{(p)} \tag{3.10}$$

where $\mathbf{D}_q^{(p)}$ is an $L_p \times M_p L_p$ matrix, representing the relating to pilots-carrying sub-carriers in $\mathbf{D}_q$. $\boldsymbol{\Delta}_q^{(p)}$ is an $M_p L_p \times M_p L_p$ diagonal matrix which is carved out of $\boldsymbol{\Delta}_q$ corresponding to the pilot-carrying sub-carriers. $\mathbf{n}^{(p)}$ stands for the noise related to pilot clusters. In (3.10), we can summarise the effect of the data from the pilots and put it with noise in a separate term $\boldsymbol{\chi}$, which characterises a disturbance to channel estimation. Let us rewrite (3.10) as a function of BEM coefficients $\boldsymbol{c}$.

$$\mathbf{y}^{(p)} = \mathbf{D}^{(p)} \mathbf{S}^{(p)} \mathbf{c} + \boldsymbol{\chi} \tag{3.11}$$

where we can collect $\mathbf{D}_q^{(p)}$ from $\mathbf{D}_q$ according to the related pilot symbols $\mathbf{y}^{(p)}$ and $\mathbf{x}^{(p)}$. We can get the integration matrix as

$$\mathbf{D}^{(p)} \triangleq [\mathbf{D}_1^{(p)}, \cdots, \mathbf{D}_{Q+1}^{(p)}], \tag{3.12}$$

and

$$\boldsymbol{S}^{(p)} \triangleq \boldsymbol{I}_{Q+1} \otimes \left(diag\left\{ \boldsymbol{x}^{(p)} \right\} \boldsymbol{F}_{L+1}^{(p)} \right), \tag{3.13}$$

where $\boldsymbol{F}_{L+1}^{(p)}$ collects the rows of $\boldsymbol{F}_{L+1}$ based on the corresponding positions of the pilots.

Applying the least squares (LS) technique, the LS estimator $\boldsymbol{W}_{LS}$ treats $\boldsymbol{c}$ as a deterministic variable. Then the BEM coefficients are estimated as

$$\widehat{\mathbf{c}} = \left\{ \mathbf{D}^{(p)} \left[\mathbf{I}_{Q+1} \otimes \left(diag\left\{ \mathbf{x}^{(p)} \right\} \mathbf{F}_{L+1}^{(p)} \right) \right] \right\}^{\dagger} \mathbf{y}^{(p)}. \tag{3.14}$$

Based on the estimated BEM coefficients $\widehat{\mathbf{c}}$ and the pre-set BEM basis, we can then reconstruct the estimated time-domain channel coefficients:

$$\widehat{\mathbf{h}}^{(t)} = (\mathbf{B} \otimes \mathbf{I}_{L+1}) \widehat{\mathbf{c}} \tag{3.15}$$

which can then be used to construct the estimate of the frequency-domain channel matrix.

3.4 Linear Equalisation

The estimated channel state information can be fully utilized by equaliser. For example, the ZF equaliser estimates the transmitted signal from the frequency-domain received signal $\mathbf{y}$ by

$$\widehat{\mathbf{x}}_{ZF} = \mathbf{W}_{ZF} \mathbf{y} \tag{3.16}$$

where the ZF equaliser is computed as

$$\mathbf{W}_{ZF} = (\widehat{\mathbf{H}}^{H} \widehat{\mathbf{H}})^{-1} \widehat{\mathbf{H}}^{H}. \tag{3.17}$$

The ZF equaliser can mitigate the ICI but may suffer from significant noise amplification, which leads to poor overall performance.

With the knowledge of the noise variance σ^2 for channel noise, the LMMSE equaliser is given by

$$\mathbf{W}_{LMMSE} = \widehat{\mathbf{H}}^H(\widehat{\mathbf{H}}\widehat{\mathbf{H}}^H + \sigma_n^2\mathbf{I})^{-1}. \tag{3.18}$$

where the term σ_n^2 can be assumed to be known based on SNR at receiver side. Simulation results will be demonstrated later to show the performance of each equaliser.

In our simulations, the system settings are as follows. We set the number of Monte Carlo simulations to be 1000, and the number of sub-carriers is fixed to $N_s = 256$. There are $M_p = 6$ equidistance pilot clusters uniformly inserted into the OFDM symbol. Each pilot cluster contains $L_p = 9$ pilot tones following the frequency-domain Kronecker Delta (FDKD) scheme [21] which contains one non-zero symbol at the cluster centre and zero symbols at both sides. This provides a guard between information carrying symbols and pilot symbols. The received symbols at the cluster centres are due to pilot symbols only and can thus be used for estimating the channel. The typical bathtub-shaped Doppler spectrum [25] is assumed. We follow the algorithm of [26] to generate the time-varying channels for the assumed Doppler spectrum. Furthermore, we assume the channel has $L + 1 = 6$ taps with normalized Doppler frequency

$$f_d \triangleq \frac{v f_c}{c} T_s N_s \tag{3.19}$$

where v denotes the velocity, f_c the carrier frequency, T_s the sampling period, and c the speed of light. $f_d = 0.2$ and $f_d = 1$ are considered in our work to represent slowly and rapidly varying channels, respectively. The channel noise is assumed to be AWGN. The time-domain received signal is shaped by the MBAE-SOE

window of [26].

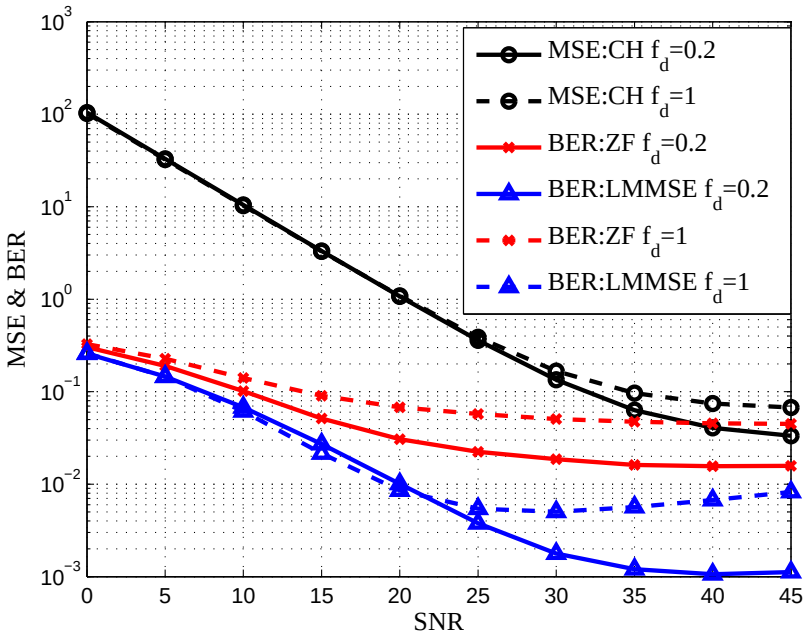

Figure 3.2: Performance of channel estimation and different linear equalisers at $f_d = 0.2$ and $f_d = 1$

Fig.3.2 shows the performance of channel estimation and different linear equalisers. As the noise information is assumed known, LMMSE equaliser delivers better performance than ZF equaliser. There is a significant degradation and trend shown for LMMSE when $f_d = 1$. It is generally caused by the channel estimation errors. And due to the fact that the "pseudocirculant" channel matrix $\boldsymbol{H}$ is extremely ill-conditioned, the noises get an amplification during the inversion of channel matrix.

The performance of the proposed system highly depends on the selection of BEM parameters and the bandwidth K of the frequency-domain channel matrix. Bad selection and assumption causes modelling error and channel estimation error and impairs the entire system.

3.5 Basis Matrix Dimension Q

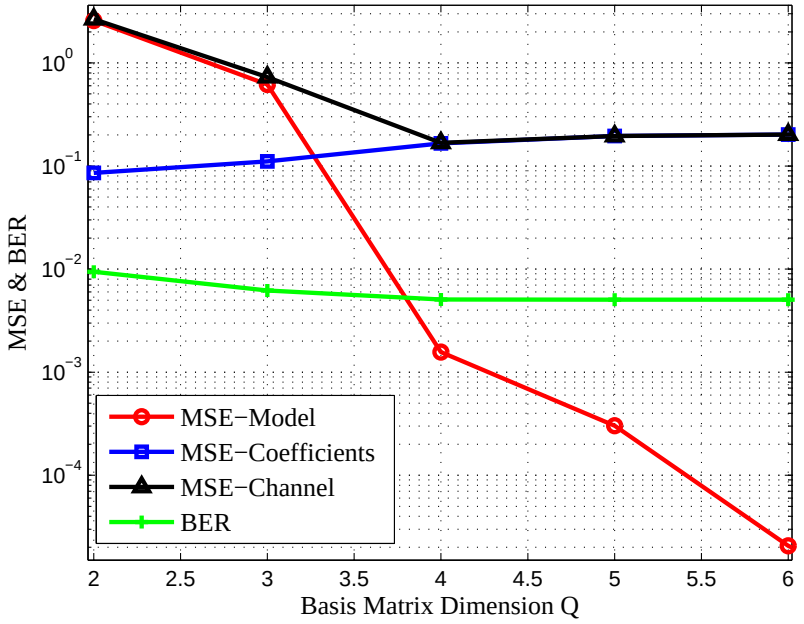

Figure 3.3: Influence of the dimension of the GCE-BEM on the modeling error, BEM coeficients estimation error, channel estimation error and bit-error rate(BER) performance of the resulting ZF equaliser.

As we discussed in the last Chapter, GCE-BEM is considering by its low modelling error. Obviously, larger basis dimensionality characterises channels for more possible changing. But it will also cost for higher computing complexity.

Fig.3.3 shows the influence of the dimensionality Q of the BEM basis. From the results, it can be seen that increasing the basis dimensionality can reduce the modelling error. However, this increases the number of BEM coefficients $\{c_{l,q}\}$ to be estimated, where the number of pilots for estimation are definite. Therefore, it can degrade the quality of estimation given the fixed number of observations on the pilot sub-carriers. As a consequence, the overall channel estimation performance first improves as Q increases due to the improved modelling accuracy but then degrades as Q increases due to the less accurate estimates of the BEM coefficients.

It is shown that $Q = 4$ is sufficient to approach the best BER performance.

3.6 Influence of Bandwidth K

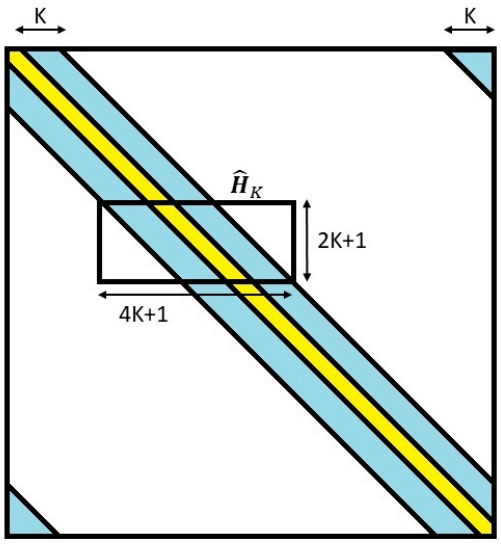

Figure 3.4: Banded Channel

In the doubly selective channel, ICI affects the channel matrix. The frequency-domain channel matrix estimate $\widehat{\mathbf{H}}$ is non-diagonal due to ICI, but the most significant entries are concentrated around the main diagonal [28]. In order to reduce computational complexity, we approximate the estimated channel matrix as a banded matrix as

$$\widehat{\mathbf{H}}_Z = \widehat{\mathbf{H}} \odot \mathbf{Z}_K, \tag{3.20}$$

where $\mathbf{Z}_K$ is a $N_s \times N_s$ matrix whose main diagonal, K sub-diagonals and K super-diagonals are all ones, with the remaining entries being zero.

We also consider the influence of the bandwidth K of the frequency-domain channel matrix estimate. In general, a higher K is needed to account for the more significant ICI in a more rapidly varying doubly selective channel with a higher f_d. But the disadvantage is causing a higher signal processing complexity.

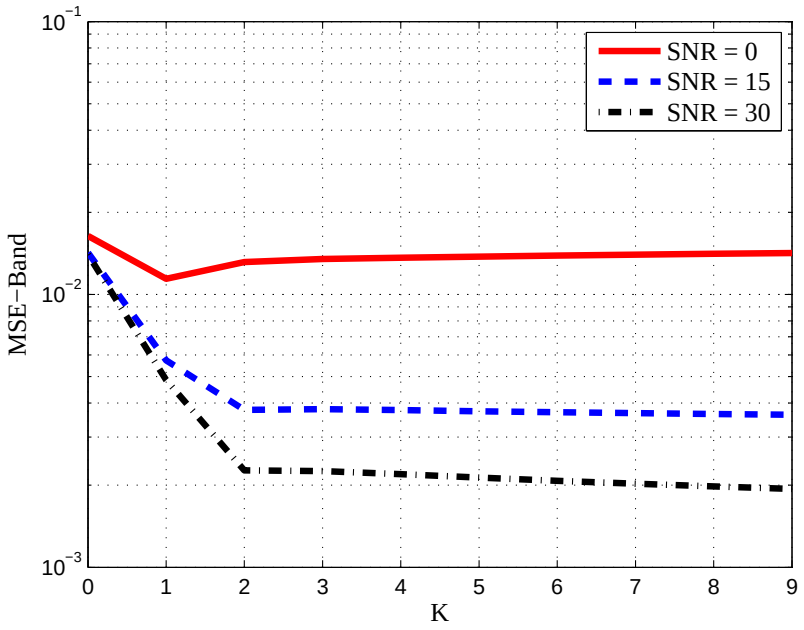

Figure 3.5: Influence of the bandwidth K of the frequency-domain channel estimates for MSE-Band at $f_d = 1$.

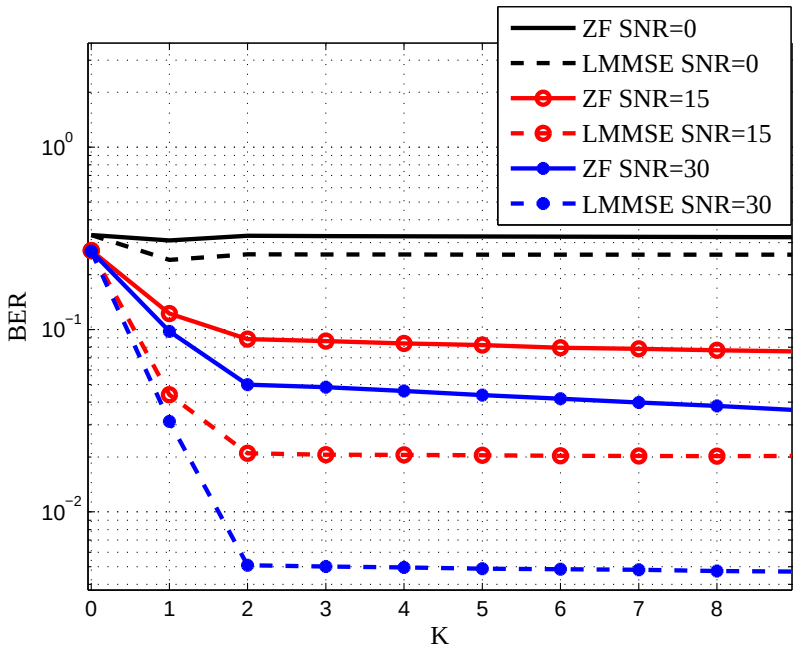

Figure 3.6: Influence of the bandwidth K of the frequency-domain channel estimates on the performance of equalisation at $f_d = 1$.

Applying window to the time-domain received signal can alleviate ICI and thus reduce the bandwidth K needed for modelling the ICI. We define the banding approximate errors by MSE-Band $\triangleq \mathbb{E}\left\{\left\|\boldsymbol{H}-\widehat{\mathbf{H}}_Z\right\|^2\right\}$. Fig.3.5 shows the relation between banding approximate errors and bandwidth K. Further, from Fig.3.6, a small value of K is sufficient for different Doppler frequencies for optimising the BER. In order to achieve a good performance-complexity trade-off, we choose $K = 2$ in the following.

3.7 Conclusion

In this Chapter, we first introduced the pilot assisted OFDM system. Combined with BEM based channel estimation, the system can re-build the CSI matrix properly, and those results can be utilised to restore the originally transmitted signal. The performance and computing complexity of the system is highly dependent on the selection of parameters, such as the BEM dimensionality Q and the banded channel bandwidth K. The simulation results show that $Q = 4$ and $K = 2$ perform well.

Chapter 4

Regularised Equalisation Based on Channel Estimation

4.1 Introduction

In this Chapter, we firstly introduce non-linear equaliser to the target system. A sorted QR decomposition method is adopted to implement the successive interference cancellation (SIC). Secondly, we introduce the regularised equaliser for both linear and non-linear systems. After that, we propose a segment-by-segment scheme aimed to reduce the computing complexity as the number of sub-carriers N_s could be a large number in the OFDM system.

4.2 Successive Interference Cancellation

Successive interference cancellation (SIC) has been extensively used in wireless communication systems to estimate transmit signals. By exploiting knowledge from the already detected symbols, their contribution can be subtracted from the received signal. This step can eliminate the interference and benefit the detection

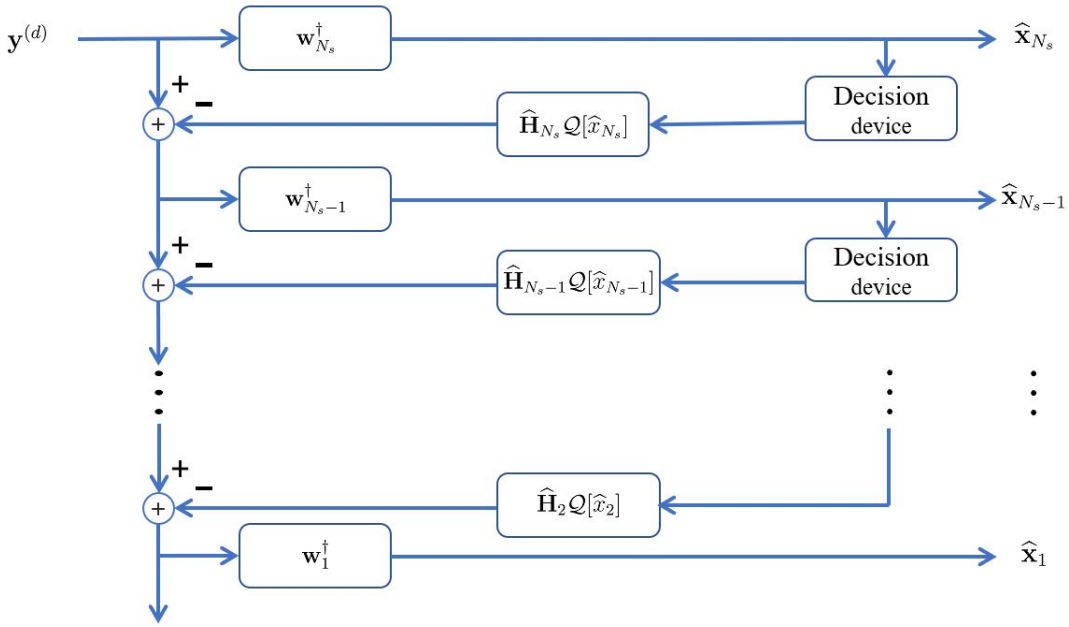

Figure 4.1: SIC detector for a block transmission scheme.

of the remaining transmit symbols.

As Fig.4.1 illustrated, a SIC detector estimates the transmit OFDM symbol $\boldsymbol{x}$ successively. x_i denotes the i-th sub-carrier of the OFDM symbol $\boldsymbol{x}$. Hard decisions on each estimated result $\mathcal{Q}[\widehat{x_i}]$ shall be used to cancel interference before the estimation for remaining data.

Furthermore, in order to improve performance, SIC based on QR decomposition (QRD) can be used. This can be done by firstly finding the QRD of the channel matrix,

$$\widehat{\mathbf{H}}_Z = \mathbf{QR} \tag{4.1}$$

where $\mathbf{Q}$ has orthogonal columns with a unit norm and $\mathbf{R}$ is upper triangular. Multiplying the received signal $\mathbf{y}$ with $\mathbf{Q}^H$ yields

$$\widehat{\mathbf{y}} = \mathbf{Q}^H\mathbf{y} = \mathbf{Rx} + \eta. \tag{4.2}$$

As $\mathbf{Q}$ is an unitary matrix, the statistical properties of the noise term $\eta = \mathbf{Q}^H\mathbf{n}$

remain unchanged. Due to the upper triangular structure of $\mathbf{R}$, the n_s-th element of $\widehat{\mathbf{y}}$ is given by

$$\widehat{y}_{n_s} = r_{n_s,n_s} \cdot x_{n_s} + \sum_{i=n_s+1}^{N_s} r_{n_s,i} \cdot x_i + \eta_{n_s} \tag{4.3}$$

and is free of interference from $x_1, \cdots, x_{n_s-1}$. Assume a descending detection order, i.e., x_{N_s} is estimated first, followed by x_{N_s-1}, etc. The decision-feedback estimate of x_{n_s} is then given by

$$\widehat{x}_{n_s} = \frac{1}{r_{n_s,n_s}} \left(\widehat{y}_{n_s} - \sum_{i=n_s+1}^{N_s} r_{n_s,i} \cdot Q[\widehat{x}_i] \right), \tag{4.4}$$

where $Q[\widehat{x}_i]$ denotes decision of $\widehat{x}_i$ according to the constellation of x_i. The detection order is crucial due to the risk of decision error and error propagation. It can be modified by permuting elements of $\mathbf{x}$ and the corresponding columns of $\mathbf{H}_Z$ prior to the QR decomposition, leading to the sorted QRD (SQRD)-based non-linear equalisation [24] [29].

4.3 Adapted Regularised Equalisation

Both the linear ZF and SQRD-based DFE can perform poorly when the channel is ill-conditioned, and the channel noise or channel estimation errors are significant.

One useful way of improving performance by solving such ill-posed problems is by applying regularisation techniques. For the ZF equaliser, a regularisation design can be realised by adding a diagonal loading factor to the Gram matrix of (3.17) and estimate $\mathbf{x}$ as

$$\widehat{\mathbf{x}} = (\widehat{\mathbf{H}}_Z^H \widehat{\mathbf{H}}_Z + \rho \mathbf{I})^{-1} \widehat{\mathbf{H}}_Z^H \mathbf{y}, \tag{4.5}$$

where ρ is the regularisation parameter. This approach has the same spirit as diagonal loading (DL) and the shrinkage approach to covariance matrix estimation.

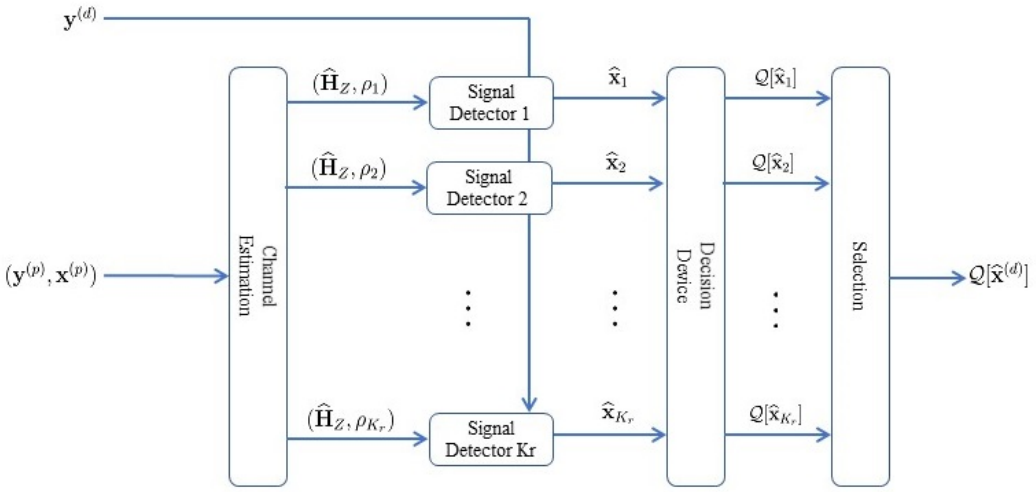

Figure 4.2: Adaptive regularised equaliser scheme.

Similar treatments have been widely used for various linear inverse problems. The parameter ρ must be chosen properly to achieve a good trade-off between bias and variance of the signal estimation such that the overall performance can be improved.

As Fig.4.2 shows, the proposed regularised approach to improve the robustness of pilot-assisted OFDM receivers mainly includes two steps:

1) Generate a set of candidate estimates of diagonal loading factors $[\rho_1, \rho_2, \cdots, \rho_{K_r}]$. Then construct the equaliser based on each diagonal loading factor.

2) Among those candidate equalisers, adaptively choose the one that leads to the best detection performance for each instantaneous received symbol based on appropriate selection approach.

In this way, a better performance may be achieved at the cost of increased complexity.

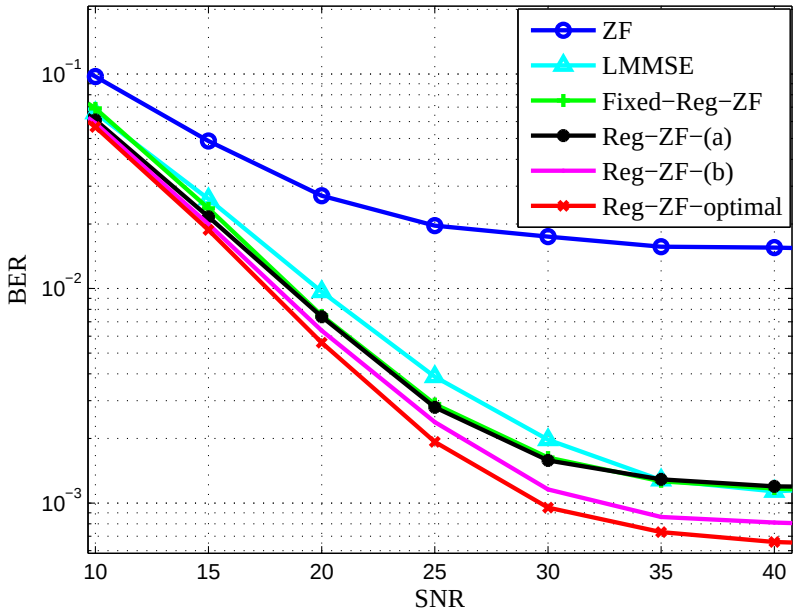

Figure 4.3: Adapted regularised equaliser with different diagonal loading set and selection at $f_d = 0.2$.

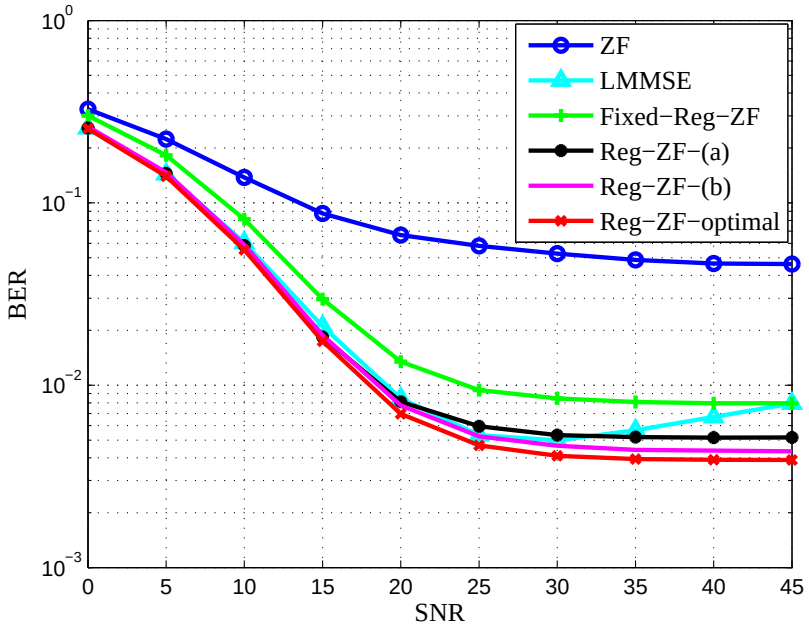

Figure 4.4: Adapted regularised equaliser with different diagonal loading set and selection at $f_d = 1$.

It is difficult to find a closed-form expression of ρ. Instead, we set a candidate set with dimension K_r as $\rho \in [\rho_1, \rho_2, \cdots, \rho_{K_r}]$ and use each candidate to produce a candidate estimate $\widehat{\mathbf{x}}_\rho$ of the transmitted signal $\mathbf{x}$ and find the decision based on the constellation used. Two diagonal loading factor selecting principles are shown as below:

$$\rho_{(1)}^* = \text{argmin}_\rho \left\| \widehat{\mathbf{x}}_\rho - Q[\widehat{\mathbf{x}}_\rho] \right\|^2, \tag{4.6}$$

$$\rho_{(2)}^* = \text{argmin}_\rho \left\| \mathbf{y} - \widehat{\mathbf{H}}_Z Q[\widehat{\mathbf{x}}_\rho] \right\|^2. \tag{4.7}$$

where $\mathbf{y}$ is received signal and $\widehat{\mathbf{H}}_Z$ is the estimated channel matrix. $\widehat{\mathbf{x}}_\rho$ and $Q[\widehat{\mathbf{x}}_\rho]$ are the detected sequences before and after a hard decision-directed adaptation. Therefore, the optimal parameter can be then chosen by minimising the difference of the estimated signal before and after the hard decision as (4.6) shows, or use (4.7) to minimize the residual of fitting the decision of transmit signal into the frequency-domain system model.

We now show the BER performance with different equalisation designs. As discussed before, adaptively selecting the regularisation parameter can improve performance. In this section, we set the dimension $K_r = 5$ and candidates of the regularisation parameter as $\{10^{-1}\lambda, 10^{-2}\lambda, 10^{-3}\lambda, 10^{-4}\lambda, 10^{-5}\lambda\}$, where λ is the average of the diagonal entries of the Gram matrix $\widehat{\mathbf{H}}_Z^H \widehat{\mathbf{H}}_Z$, which is also equal to the average of the eigenvalues of $\widehat{\mathbf{H}}_Z^H \widehat{\mathbf{H}}_Z$.

Firstly, we will discuss the influence of the set of candidate diagonal loading factors.

Fig.4.3 and Fig.4.4 show the simulation results for linear ZF equaliser. We also compare the performance achieved with the fixed chosen regularisation factor, the optimally chosen regularisation parameters (chosen by real BER for each candi-

date, which is unable to achieve in practice) and that with the practical parameter choice of (4.6) and (4.7). It can be seen that for both slowly and rapidly varying channels, regularisation can significantly improve the performance. Their closeness indicates that the gain of regularisation can indeed be claimed in practice.

For the selection from candidate detectors, both figures show that selection (4.7) perform better efficiency compared with (4.6), and it achieves the parallel performance with the optimal selection which is not practicable as the real BER is unknown. However, (4.7) leads to higher computing complexity compared with (4.6).

The above regularisation design can be extended to the non-linear DFE based on QRD. In this case, instead of finding the QR decomposition of $\widehat{\mathbf{H}}_Z$, we perform the QR decomposition of the extended channel matrix

$$\begin{bmatrix} \widehat{\mathbf{H}}_Z \\ \sqrt{\rho}\mathbf{I}_{N_s} \end{bmatrix} = \begin{bmatrix} \mathbf{Q}_1 \\ \mathbf{Q}_2 \end{bmatrix} \mathbf{R}. \tag{4.8}$$

The equalisation process then follows the same way as in (4.2)-(4.4) by using $\mathbf{Q}_1$ and $\mathbf{R}$. Similarly, we can optimize the estimation order by finding an optimized permutation matrix using the SQRD algorithm [29]. Note that in the regularised designs, the regularisation parameter ρ is adaptively chosen to account for the instantaneous realizations of noise, ICI and error due to channel estimation, which are time-varying and unknown to the receiver (even their statistics may be obtainable when the statistical model of the system is known).

Fig.4.5 and Fig.4.6 show the BER performance of regularised SQRD equalisation. Due to the channel estimation errors and ill-conditioned channel matrix, the typical SQRD equaliser suffers significant degradation. The adapted regu-

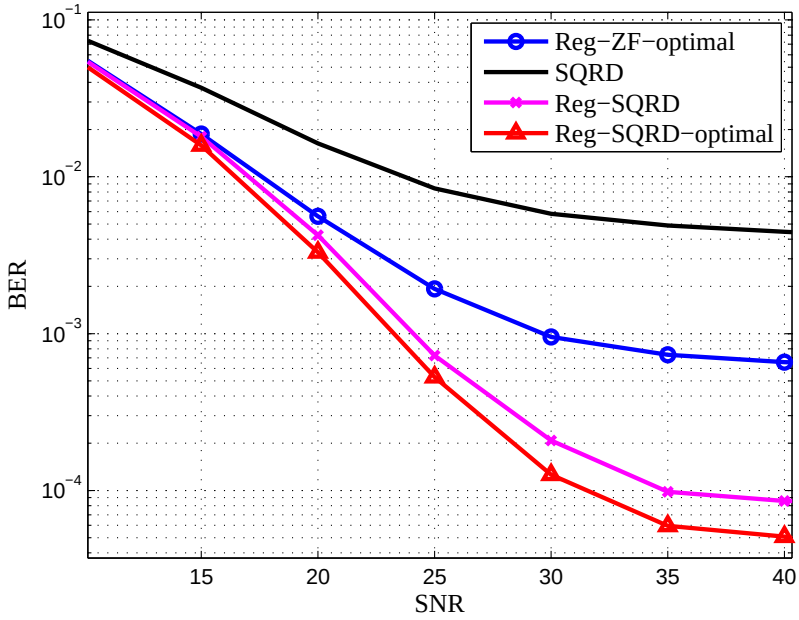

Figure 4.5: BER performance with adaptive regularised SQRD equalisation for fd=0.2.

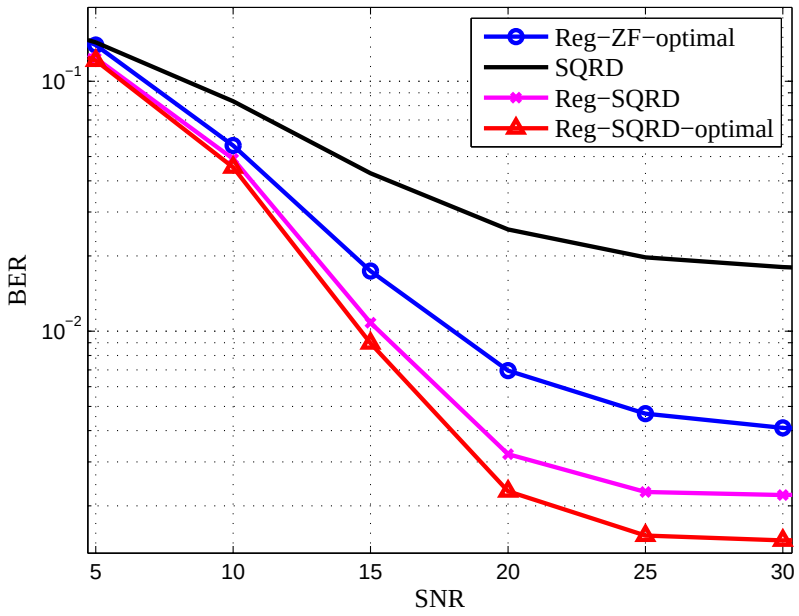

Figure 4.6: BER performance with adaptive regularised SQRD equalisation for fd=1.

larised SQRD equalisation based on selection (4.7) is illustrated to compare with the traditional SQRD and optimal adapted SQRD (candidate detector selected by real BER). The results show that the proposed adapted regularisation bringing significant performance gain to SQRD equaliser.

4.4 Segment-by-Segment Equalisation

In OFDM systems, the number of sub-carriers N_s could be a large number, which results in a high computational complexity of equalisation in doubly selective channels. Recall that clustered pilots are used for estimating the channel due to ICI, which naturally divide the overall received signal into multiple K_m segments, and each can be used for recovering a segment of the transmitted symbols with low interference from other segments. In this case, a segment-by-segment strategy with segments separated by the pilot clusters, as $K_m = M_p + 1$, can be used for equalisation and the overall complexity can be reduced. We may further decrease the size of each segment for further complexity reduction.

We also show the performance of segment-by-segment equalisation in Fig.4.7 and Fig.4.8. Two designs are compared: 1) the overall equalisation scheme based on the entire received signal and full channel matrix; 2) the segment-by-segment equalisation with segments separated by pilot clusters. It is seen that, in addition to the complexity advantage, segmentation can slightly improve the performance of regularised equalisation, which may be attributed to that the regularisation parameters are adapted to each segment.

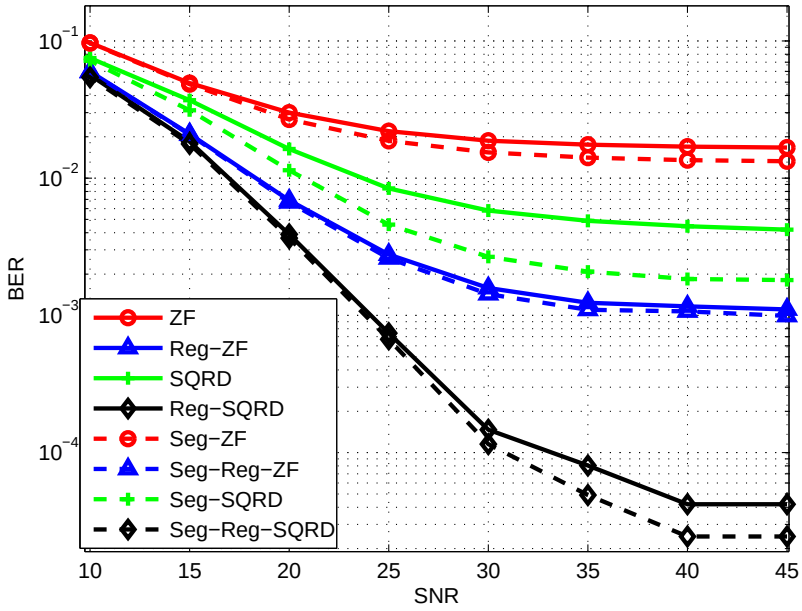

Figure 4.7: BER performance with different schemes with fd=0.2.

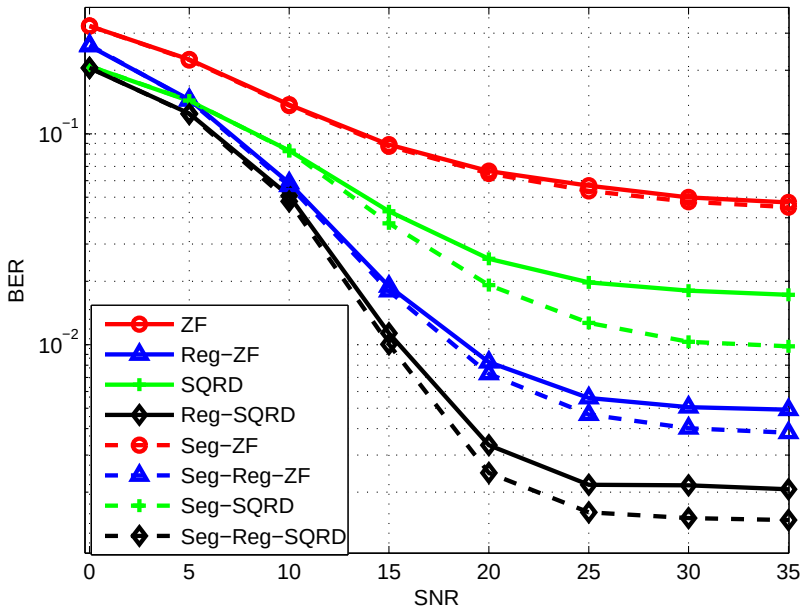

Figure 4.8: BER performance with different schemes with fd=1.

4.5 Conclusion

In this Chapter, we proposed a new high-efficiency regularised approach and a low-complexity segment-by-segment approach for both linear ZF equalisation and non-linear SQRD equalisation. The adapted selection considers the residual of fitting the decision to transmit signal into the estimated CSI, and chooses the proper data from the set of candidates. These selections can be extended to the separated segments. The simulation results show improved performance with lower complexity compared to existing systems.

Chapter 5

Conclusions and Future Work

5.1 Conclusions

In this thesis, we investigated the performance of OFDM systems employing BEM-based channel estimation. We firstly discussed the effects of the dimension for basis matrix and the bandwidth of the frequency-domain channel matrix. Both parameters can set to proper value to achieve good trade-off between performance and complexity. After that, we considered linear and non-linear equalisers and introduced regularisation schemes to enhance the performance. The proposed adaptive-selection of regularised equalisation improves performance compared with non-regularised schemes. At last, we proposed a segment-by-segment scheme for both linear and non-linear equalisation to reduce the computational complexity, especially when the duration of each symbol is quite large.

To sum up, in this thesis, we mainly focus on channel estimation and equalisation schemes for BEM based OFDM systems. The numerical results indicated that the proposed regularisation and segment-by-segment equalisation schemes

achieved better performance compared with existing approaches.

5.2 Future Work

The present work focuses on single-input single-output communications with single users. The methods proposed in this work shall be extended to more general cases, e.g., with multiple antennas and multiple users. Furthermore, the methods may be adapted for emerging waveforms for future-generation wireless communications.

References

[1] A. Goldsmith, *Wireless communications / Andrea Goldsmith.* Cambridge University Press, 2005.

[2] T. Hwang, C. Yang, G. Wu, S. Li, and G. Y. Li, "OFDM and its wireless applications: A survey," *IEEE Transactions on Vehicular Technology*, vol. 58, no. 4, pp. 1673–1694, May 2009.

[3] B. Farhang-Boroujeny and H. Moradi, "OFDM inspired waveforms for 5g," *IEEE Communications Surveys Tutorials*, vol. 18, no. 4, pp. 2474–2492, Fourthquarter 2016.

[4] P. Fan, E. Panayirci, H. V. Poor, and P. T. Mathiopoulos, "Special issue on broadband mobile communications at very high speeds," *EURASIP Journal on Wireless Communications and Networking*, vol. 2012, no. 1, p. 279, Aug 2012.

[5] Z. Tang, R. C. Cannizzaro, G. Leus, and P. Banelli, "Pilot-assisted time-varying channel estimation for OFDM systems," *IEEE Transactions on Signal Processing*, vol. 55, no. 5, pp. 2226–2238, May 2007.

[6] K. V. Vardhan, S. K. Mohammed, A. Chockalingam, and B. S. Rajan, "A

low-complexity detector for large MIMO systems and multicarrier CDMA systems," *IEEE Journal on Selected Areas in Communications*, vol. 26, no. 3, pp. 473–485, April 2008.

[7] S. S. Haykin and M. Moher, *Modern wireless communications / Simon Haykin and Michael Moher.* Pearson Prentice Hall, 2005.

[8] T. S. Rappaport, *Wireless communications : principles and practice / Theodore S. Rappaport.* IEEE Press, 1996.

[9] T. S. Rappaport *et al.*, *Wireless communications: principles and practice*. prentice hall PTR New Jersey, 1996, vol. 2.

[10] R. W. Chang, "Synthesis of band-limited orthogonal signals for multichannel data transmission," *The Bell System Technical Journal*, vol. 45, no. 10, pp. 1775–1796, Dec 1966.

[11] B. Saltzberg, "Performance of an efficient parallel data transmission system," *IEEE Transactions on Communication Technology*, vol. 15, no. 6, pp. 805–811, December 1967.

[12] S. Weinstein and P. Ebert, "Data transmission by frequency-division multiplexing using the discrete fourier transform," *IEEE Transactions on Communication Technology*, vol. 19, no. 5, pp. 628–634, October 1971.

[13] A. Peled and A. Ruiz, "Frequency domain data transmission using reduced computational complexity algorithms," in *ICASSP '80. IEEE International Conference on Acoustics, Speech, and Signal Processing*, vol. 5, April 1980, pp. 964–967.

[14] E. N. Committee *et al.*, "Radio broadcasting systems, digital audio broadcasting (dab) to mobile, portable and fixed receivers," *Norme ETSI, Sophia-Antipolis, France, Doc. ETS*, vol. 300, no. 401, pp. 1995–1997, 1995.

[15] L. T. Berger, A. Schwager, P. Pagani, and D. Schneider, *MIMO power line communications: narrow and broadband standards, EMC, and advanced processing*. CRC Press, 2014.

[16] F. Schaich and T. Wild, "Waveform contenders for 5gofdm vs. fbmc vs. ufmc," pp. 457–460, 2014.

[17] M. Oltean, "An introduction to orthogonal frequency division multiplexing," *Analele Universitatii Oradea, 2004, Fascicola Electrotehnica, Sectiunea Electronica*, pp. 180–185, 2004.

[18] M. K. Tsatsanis and G. B. Giannakis, "Modelling and equalization of rapidly fading channels," *International journal of adaptive control and signal processing*, vol. 10, no. 2-3, pp. 159–176, 1996.

[19] D. K. Borah and B. T. Hart, "Frequency-selective fading channel estimation with a polynomial time-varying channel model," *IEEE Transactions on Communications*, vol. 47, no. 6, pp. 862–873, June 1999.

[20] X. Ma, G. B. Giannakis, and S. Ohno, "Optimal training for block transmissions over doubly selective wireless fading channels," *IEEE Transactions on Signal Processing*, vol. 51, no. 5, pp. 1351–1366, May 2003.

[21] A. R. Kannu and P. Schniter, "MSE-optimal training for linear time-varying channels," in *Proceedings. (ICASSP '05). IEEE International Conference on Acous-*

tics, Speech, and Signal Processing, 2005., vol. 3, March 2005, pp. iii/789–iii/792 Vol. 3.

[22] P. J. Bickel, B. Li, A. B. Tsybakov, S. A. van de Geer, B. Yu, T. Valdés, C. Rivero, J. Fan, and A. van der Vaart, "Regularization in statistics," *Test*, vol. 15, no. 2, pp. 271–344, 2006.

[23] A. Neumaier, "Solving ill-conditioned and singular linear systems: A tutorial on regularization," *SIAM review*, vol. 40, no. 3, pp. 636–666, 1998.

[24] J. Tong, L. Li, Q. Guo, P. J. Schreier, and J. Xi, "Regularized successive interference cancellation (SIC) under mismatched modeling," in *2014 IEEE Workshop on Statistical Signal Processing (SSP)*, June 2014, pp. 328–331.

[25] W. C. Jakes, *Mobile Radio Systems*. IEEE, 1974.

[26] Y. R. Zheng and C. S. Xiao, "Simulation models with correct statistical properties for rayleigh fading channels," *IEEE Transactions on Communications*, vol. 51, no. 6, pp. 920–928, June 2003.

[27] M. Visintin, "Karhunen-loeve expansion of a fast rayleigh fading process," *Electronics Letters*, vol. 32, no. 18, pp. 1712–, Aug 1996.

[28] J. Wu and P. Fan, "A survey on high mobility wireless communications: Challenges, opportunities and solutions," *IEEE Access*, vol. 4, pp. 450–476, 2016.

[29] D. Wubben, R. Bohnke, V. Kuhn, and K. . Kammeyer, "Mmse extension of v-blast based on sorted qr decomposition," in *2003 IEEE 58th Vehicular*

Technology Conference. VTC 2003-Fall (IEEE Cat. No.03CH37484), vol. 1, Oct 2003, pp. 508–512 Vol.1.